Project ? 1777p

Theoretical studies of scaling double-clad fiber lasers to high power

Report for the period from 01/04/2000 to 30/06/2001 (Final Report)

Duration of the Project: April 2000 – June 2001

Project Manager: V. D. Soloviev
St. Petersburg, Kuznecova Pr. 29 Building 2, Ap. 135
Tel: (812) 151-68-00
Fax: (812) 5524672
E-mail: vdsol@mail.axon.ru

St. Petersburg State Technical University

REPORT DOCUMENTATION PAGE

Form Approved OMB No. 0704-0188

1. REPORT DATE *(DD-MM-YYYY)*	2. REPORT TYPE	3. DATES COVERED *(From – To)*
24-07-2001	Final Report	01/04/2000 - 23-Aug-01

4. TITLE AND SUBTITLE

Theoretical Studies of Scaling Double Clad Fiber Lasers to High Power

5a. CONTRACT NUMBER
ISTC Registration No: 1777

5b. GRANT NUMBER

5c. PROGRAM ELEMENT NUMBER

6. AUTHOR(S)

Professor Yuri Anan'ev

5d. PROJECT NUMBER

5d. TASK NUMBER

5e. WORK UNIT NUMBER

7. PERFORMING ORGANIZATION NAME(S) AND ADDRESS(ES)

St. Petersburg State Technical University
Polytechnicheskaya 29,
St. Petersburg 195251
Russia

8. PERFORMING ORGANIZATION REPORT NUMBER

N/A

9. SPONSORING/MONITORING AGENCY NAME(S) AND ADDRESS(ES)

EOARD
PSC 802 BOX 14
FPO 09499-0014

10. SPONSOR/MONITOR'S ACRONYM(S)

11. SPONSOR/MONITOR'S REPORT NUMBER(S)
ISTC 99-7005

12. DISTRIBUTION/AVAILABILITY STATEMENT

Approved for public release; distribution is unlimited.

13. SUPPLEMENTARY NOTES

14. ABSTRACT

Ytterbium (Yb) - doped fiber lasers have demonstrated efficient optical-to-optical continuous-wave power conversion into a diffraction-limited laser beam. Power scaling these devices has benefited from recent dual-clad fiber designs that specifically allow improved coupling of diode-laser emission and interaction with the Yb-doped core. To realize efficient, kilowatt-scaleable, Ytterbium-doped fiber laser designs many limiting factors must be better understood. The research on this project will consist of the theoretical study of fiber lasers in general, and dual-clad Ytterbium-doped fiber lasers specifically, in order to provide a sound, comprehensive foundation for understanding these devices.

15. SUBJECT TERMS
EOARD, Physics, Optics

16. SECURITY CLASSIFICATION OF:			17. LIMITATION OF ABSTRACT	18, NUMBER OF PAGES	19a. NAME OF RESPONSIBLE PERSON
a. REPORT	b. ABSTRACT	c. THIS PAGE			Dr. Alexander J. Glass, EOARD
UNCLAS	UNCLAS	UNCLAS	UL	63	19b. TELEPHONE NUMBER *(Include area code)* +44 20-7514-4953

Contents

Introduction

The recent years have been witnessing explosive development of diode-pumped double-clad fiber lasers (see, e.g., [1]). Being very compact and highly efficient, these lasers start finding application not only in such areas traditional for fiber lasers as communication and information processing systems, but in high-energy materials processing as well. The point is that the output power obtainable from these lasers has been increasing year after year, to reach presently an impressive level. For instance, while in 1993 producing 0.75 W in the single-mode regime [2] was considered a big achievement, only a few years later some experimenters succeeded in delivering tens of watts of output power (for example, a power of 40 W was reported to have been produced in 1997 [3]).

The first place among double-clad lasers is presently occupied by devices whose core (made of quartz) is doped by ytterbium [4--8]. There are a number of reasons for this. First, ytterbium has very broad absorption (800 to 1064 nm) and emission (970--1200 nm) bands. Also, the level diagram is such as to practically exclude multiphoton nonradiative decay of the excited state, absorption from the latter, and concentration quenching.

Besides, one achieves here readily oscillation at a number of wavelengths lying comparatively close to those of pumping. For instance, by pumping at 975 nm one can obtain coherent emission at 1020 nm; one can add two more pairs of such wavelengths, namely, 1064 and 1120 nm and 900 and 975 nm. In all these cases, the difference between the pump and oscillation photon energies, which is responsible for the heat released in the host material, is only one third that obtained when using such a popular dopant as neodymium. All these factors favor achieving a high efficiency of frequency conversion when employing for a primary source either some semiconductor or YAG lasers.

Progress in producing gratings written directly into fibers [9] brought closer to solution the problem of obtaining single-frequency oscillation tunable within a broad range. On the other hand, the large width of the emission spectra makes possible generation of ultrashort pulses and using such lasers in a variety of devices based on nonlinear optics.

The present work analyses the possibilities of further increasing the output power of double-clad lasers. It also considers the prospects of developing methods permitting frequency conversion of the radiation generated by these lasers, which are needed for the numerous practical applications. It should be pointed out that most of the publications dealing with lasers of this kind describe only small-step technical improvements and the attendant improvement of the laser performance achieved in the various regimes. There are comparatively few papers devoted to problems of basic significance, and it is these papers that we shall pay attention here to.

Energy Characteristics of the Radiation

Nearly every paper dealing with the problem of increasing the fiber-laser output power mentions the various mechanisms placing a constraint on the latter. They are listed as follows [2]:

1. Fiber propagation loss

2. Amplified spontaneous emission and/or parametric amplification or oscillation

3. Thermal effects (heating, quenching, lensing)

4. High intensity nonlinear effects (self-focusing, Raman and Brillouin gain)

5. Surface damage to laser mirrors. Optical breakdown of glass .

The first three of the above mechanisms turn out to have approximately the same significance in all possible regimes of fiber laser operation, and therefore they deserve a comprehensive consideration. As for nonlinear effects and degradation of optical components, their probability increases sharply with increasing peak power of the radiation. For the same average radiation power, quasisteady-state operation is achieved at the lowest peak power, and therefore it is in this regime that one obtains the highest average power levels, and it is its theory that we are primarily going to consider here.

Practically all authors use in describing the quasisteady-state regime models of varying degrees of complexity, which are based on inverse-population and photon-balance equations. The simplest and, historically, the first consideration of the energy characteristics of a fiber laser was presented in the publication of Koestler and Snitzer [10]. It dealt with laser operation in the small-signal low-gain regime. Viewed from the energy efficiency standpoint, this regime is unattractive, because during the time the signal remains weak in the beginning of its propagation along the amplifier it cannot use in full measure the available inverse population. For this reason we are going to focus our attention in what follows on oscillation with a much more uniform distribution of the total coherent radiation over the laser length.

One of the most adequate models for the quasisteady-state lasing regime was proposed in [11]. This paper presented a calculation of the spatial competition among various waveguide modes, made with due account of gain saturation in the presence of these modes. The medium was assumed to be a four-level material with the unpopulated lowest operating level (this was not specified by the authors but can be inferred from the calculations). One took into account not only the field distribution configuration of the individual modes but the nonuniformity of pumping distribution over the fiber cross section. We may recall that a similar model was proposed in its starting version as far back as the 1960s by Tang and Statz [12, 13]; it was soon generalised by Russian authors to the case of signals considerably in excess of the threshold for laser action [14--16] through expansion in the saturation parameter. The same approach was employed in [11]. One shortcoming of [11] and of some other Western studies devoted to the calculation of transverse-mode competition lies in using an azimuthal factor of the type of $\cos(m\varphi)$, where φ is the azimuthal angle, and m is an integer (azimuthal index), in the field distributions of these modes. In actual fact, as this was shown by us in [19], one can use to advantage the point that in axially symmetric systems the modes with factors of the type of $\cos(m\varphi)$ and $\sin(m\varphi)$ are degenerate, and therefore their superpositions $\cos m\varphi \pm i \sin m\varphi = e^{\pm im\varphi}$, whose intensity does not depend on the radial angle, are also modes

of the system. It is using the latter modes in calculations of mode competition that will permit us to restrict ourselves subsequently to the solution of a one-dimensional problem taking into account the dependencies of all the distributions on the radial direction only. We note finally that the calculations in [11] were led to the end only for the case of single-mode oscillation, whereas the present Project envisages a consideration of the multi-mode regime as well, a problem which is particularly important for an analysis of the possibilities of scale-up and is much more complex. This complication of the problem can be compensated to a certain extent by the fact that one will possibly be able to limit oneself to the case of uniform pumping distribution over the core cross section (which immediately makes the calculations more general). The point is that because of the small jump in the refractive index the pump launched into the core undergoes only an insignificant refraction at its side surface and, on entering the core, is weakly absorbed in it because of its small diameter. Thus the effects which in conventional solid-state lasers give rise to a substantial nonuniformity of pump distribution over the cross-sectional area of the active element [20], here should be much weaker.

The actual method of pumping chosen and a proper selection of the resonator scheme play a prominent part in achieving a high energy conversion efficiency. Although many researchers use side pumping (see, e.g., [21, 22]), direct end-launching of co-propagating pump is employed most frequently. The dopant is usually contained in a core of such a small diameter that only a few waveguide modes (most frequently, one) are involved in the gain or oscillation regime, and the pump radiation is launched into the inner cladding, which has a much larger area. The pump crosses many times the core, and it is here that it is predominantly absorbed. This approach permits one to strongly increase the pumping level compared to the case of its direct launching into the narrow fiber core. To use the pump to the full extent, one either deposits on the resonator output mirror a coating which is almost fully reflecting at the pump frequency [2] or uses a fiber long enough to achieve practically complete absorption of the pump radiation [23].

It is the co-propagating pumping that is used and analysed in most cases. We believe it appropriate to consider here also the case of end-pumping from both sides of the waveguide, which should provide the highest possible output power and conversion efficiency; to the best of our knowledge, this approach has not been treated in the literature. In this case, a beam-splitting mirror reflecting the signal toward the resonator output mirror and transmitting the pump radiation should be placed at the output end of the core. Such a mirror should possess practically the same parameters as the mirrors usually deposited on the opposite end of a waveguide. For instance, the mirror employed in [2] had a reflectivity for the pump less than 1%, and for the laser radiation, above 99%. This solution is argued for by the following reasoning. Oscillation in ytterbium proceeds by the three-level diagram, and the parts of the waveguide that are doped but not pumped to the full extent not only amplify but absorb the laser radiation as well. Pumping the waveguide from the second end as well increases noticeably the uniformity of pump distribution over the length and precludes formation of absorbing regions. Note also that the laser radiation flux reaches its maximum level near the output mirror, and therefore increasing the pump density in this zone should produce a particularly favourable impact on the laser energy efficiency.

One of the most complex problems in calculating and designing double-clad lasers is the choice of the shape of the inner cladding and taking into account its effect on the effective pump-absorption coefficient. The only paper presenting a comprehensive analysis of this issue is Ref. [25]. These calculations provided supportive data for an earlier suggestion that the coaxial waveguide geometry (the central core and the first cladding are circular coaxial cylinders) is unfavourable from the standpoint of efficient use of the pumping. The fact is that the pump propagates primarily through the peripheral zone of the circular cladding, past the doped core.

The most complex calculations made in three dimensions showed that the always present bend in the fiber improves the situation but not well enough. A substantially larger increase of the fraction of pump energy launched into the core is reached when the first cladding, while retaining its circular shape, is displaced noticeably with respect to the former. A similar effect is observed when one crosses over from the circular to rectangular cross section. In this case the effective pump absorption coefficient along the fiber approaches that in the core multiplied by the ratio of its area to that of the inner cladding; it is this approximation that is used in most of the corresponding estimates. As for the shape of the inner cladding, one follows presently the recommendations of [26] and uses most frequently a close to square cross section [27, 23]. This shape provides both a satisfactory pump absorption coefficient and convenient end-launching of the pump into the core.

We shall dwell now briefly on the factors capable of reducing the output power of the lasers under consideration or of imposing on it fundamental constraints. We start with heat dissipation in the fiber. Most of the studies stress the point that because of the extremely developed surface area of the gain medium, fiber lasers are much less subject to thermal effects than the conventional types. The corresponding estimates reported in [2] lend support to this general relation. They covered the following effects:

1. Thermal stress in the fiber which, for high pump power, leads to fracture; this effect sets an upper bound to the maximum amount of heat that may be dissipated in a fiber laser

2. A decrease in quantum efficiency caused by the temperature deactivating of exited state

3. Distortion of the refractive index step-profile of the fiber and changes of the fiber mode number through the temperature dependence of the core radius and refractive index and through the photo-elastic effect

4. Chemical instability of the soft fluoro-polymer that makes the second-clading

Judging from [2], the most serious of the above effects is the influence of fiber temperature on the quantum efficiency of energy conversion. Although the possible effect of superradiance on the energy characteristics of fiber lasers has been mentioned more than once, the pertinent information is very scant. An attempt at making a theoretical estimate of the power of spontaneous emission was made in [2]. The authors of [2] used an extremely strange expression by which this power does not depend even on the excited state population; therefore the results quoted in [2] in this respect can hardly be trusted. Experimental measurements of the power of amplified spontaneous emission at the exit from a fiber laser was performed in [23]; it was found that this power per 1 nm is inferior to that of lasing by 55 dB. Whence it follows that in a properly designed oscillator the part played by superradiance should not be anywhere near important.

The power constraints associated with all other possible factors (Raman scattering, self-focusing, thermal lensing, mirror degradation) were estimated more or less systematically in [2].

Frequency Conversion in Fiber-Laser Arrangements

The various present and future applications of fiber lasers in communication systems, medicine, materials processing, printing, and optical storage devices impose different requirements on their spectral characteristics. The emission spectrum of these lasers is controlled by methods both traditionally employed with bulk lasers and those developed specifically for fiber lasers. The desired emission spectrum is frequently obtained by combining several methods of control. Because these methods are fairly universal, we shall present below illustrations of their use not only for the ytterbium-doped but for other fiber lasers as well.

In a general case, when lasing at a specific wavelength within the gain band is required to obtain without resorting to spectral selection techniques, this can be done by a number of methods. To begin with, the oscillation wavelength depends on the actual pumping conditions. There is a broad variety of possible pump sources (AlGaAs and InGaAs diodes, titanium sapphire lasers, Nd:YLF and Nd:YAG lasers) with wavelengths lying from 800 to 1064 nm. Second, the wavelength can be controlled within a limited range by properly varying the resonator Q or the fiber length. All these aspects are discussed in considerable detail in [26].

The traditional method of controlling the laser emission spectrum is based on spectral selection within the medium gain bandwidth. In principle, one could use for this purpose such bulk elements as prisms and gratings together with the necessary lenses, which should be mounted inside the resonator. Besides the unavoidable inconveniences, however, these elements would introduce additional losses, thus reducing substantially the laser efficiency. A much more attractive approach to achieve laser action at any wavelength within the gain bandwidth consists in using Bragg gratings written directly into the fiber. In this case the achievable wavelengths are determined primarily by the width of the fiber gain bandwidth, because progress reached in manufacturing such gratings [9, 28, 29] solved the problem of providing the necessary frequency discrimination. Because the Yb^{3+} emission spectrum is fairly broad, particularly when using a germanosilicate host, the laser can be made to operate in the weak emission wings while providing a high enough frequency discrimination to suppress oscillation at the peak of the gain profile. One can achieve in this way narrow-band oscillation at any wavelength from 975 to 1200 nm, with a tunability of 1%. Retuning to another frequency can be done by stretching or temperature tuning the grating [26].

Optical amplification of signals in fiber-optics communication systems is the crucial part of the so-called DWDM (dense-wavelength-division-multiplexed) transmission systems. Stimulated Raman scattering (SRS) appears to hold considerable promise for this application. This phenomenon was one of the first to be studied as applied to optical amplification [30]. In SRS, the light scattered by optical vibrational modes (optical phonons) undergoes a Stokes frequency shift. In optical fibers doped by GeO_2, which changes the refractive index, this shift is 450 cm^{-1} [31]. For instance, radiation with a wavelength of 1450 nm provides amplification in the 1540--1560-nm transparency window of the fiber. Because Raman amplification is a nonlinear process, it is strongly dependent on the pump power density in the transmitting fiber. Engineers are pinning their hopes on the use for this purpose of a Raman laser which has been considered in a large number of publications.

To illustrate the operation of the Raman laser, consider the arrangement described in [32]. The first element here is a cladding-pumped fiber laser. It is pumped usually by several multimode diode lasers. The 1117-nm output of this laser is fed into the second element of the arrangement, namely, a multi-staged Raman resonator. When propagated through this resonator,

the wavelength is SRS-shifted successively up to the required value (for instance, to reach the 1450-nm range). The multi-staged Raman resonator is formed by Bragg gratings written into the fiber. By using highly-reflecting gratings for each intermediate Stokes frequency, one decreases the corresponding threshold and, thus, can achieve efficient conversion of the starting 1117-nm laser radiation through five consecutive Stokes shifts up to 1480 nm. The gratings are arranged in such a way that each subsequent Stokes component is produced actually by intracavity oscillation. This system ends in an output grating with a reflectivity of about 20% at the required wavelength. The power obtained with diode pumping at a wavelength of 1480 nm was 1.7 W at a conversion efficiency of 46% [33].

The power reached with a conventional flashlamp-pumped Nd:YAG laser as a pumping source was 2.6 W at 1480 nm. The gain bandwidth at half maximum was 2 nm. Because the Raman gain bandwidth is broad (more than 20 THz), the choice of the oscillation frequency is determined by the spectral response of the reflectivity of each Bragg grating. By properly varying the Stokes shifts in intermediate orders, one can readily produce lasing within the spectral range extending from 1.1 to 2.0 μm. The above arrangement demonstrates a high efficiency of pump frequency conversion to oscillation of the desired frequency. Besides, this arrangement provides also a good scaling capability; indeed, adding pump lasers results in a corresponding growth of output power.

The material usually employed for the nonlinear gain medium of a Raman laser is a single-mode fiber. However a multimode fiber has a number of assets in frequency conversion. One can more easily achieve with it efficient launching of pump radiation, and do it at higher powers too. As a consequence, one succeeds in producing higher-power Stokes components over a broader frequency range. For instance, Ref. [34] describes a double-transit Raman laser with a multimode fiber heavily pumped by the second harmonic of a Q-switched Nd:YAG laser. An essential component of this arrangement is a spectral selector based on a Littrow prism used in the autocollimation regime. To increase the spectral selectivity, an additional dispersion prism was employed in some cases. Experiments made on multimode fibers of various lengths demonstrated the possibility of achieving continuously tunable lasing over a broad spectral range (0.54--1.0 μm).

A Raman laser arrangement was built to amplify signals with a wavelength of 1.3 μm, which falls on one of the communication windows of present optical systems [35]. In contrast to the laser described in [32], here oscillation was achieved in a ring resonator made up only of fused wavelength-division-multiplexing (WDM) couplers [36, 37], with low-loss GeO2-doped single-mode fiber used as the active medium. High-efficiency multi-staged Raman oscillation was demonstrated up to the third Stokes component (1.12, 1.18, and 1.24 μm) when pumped by a CW Nd:YAG laser operating at 1.064 μm. Oscillation at the longer-wavelength Stokes components (1.31 and 1.38 μm) was suppressed.

A simple SRS-based laser arrangement operating at 1.24 and 1.48 μm and considered to be a promising pump source for the 1.31- μm Raman amplifier and Er-doped fiber amplifier, respectively, was proposed [38, 39]. The above studies demonstrated for the first time efficient conversion of the 1.06-μm CW radiation to the first (1.24 μm) and second (1.48 μm) Stokes components in SRS in phosphosilicate fiber. The authors stress that the Stokes shift in germanosilicate waveguide is 440 cm-1, so that to obtain the 1.24- and 1.48-μm wavelengths one has to use Stokes components of the third and sixth order, respectively. The Stokes shift in phosphosilicate waveguides is 1330 cm-1, which is three times that obtained in a germanosilicate waveguide. This made it possible to drop multi-staged SRS conversion and to obtain the desired wavelength of 1.24 μm already in the first Stokes component. In this way the

laser arrangement was considerably simplified. Apart from this, it was found possible to write high-reflecting Bragg gratings into this fiber. Improvements in the structure and technology of fabrication of phosphosilicate waveguides culminated in generating an output power of 2.4 W when pumped by a 3.5-W neodymium-doped fiber laser.

Up-conversion fiber lasers form a separate group of lasers operating in the visible [15]. They compete with ion and metal-vapor lasers. Achieving oscillation by up-conversion means essentially that two infrared photons absorbed in a medium produce in the final count one photon in the visible range. Considered from the physical standpoint, the excitation occurs through a stepped transition of the system to the upper energy level through an intermediate state. Subsequent emission can be produced in transitions to levels lying from the intermediate to the ground state.

The Pr3+ ion has a close-to-ideal level structure permitting one to reach the upper excited state by absorbing a 850-nm photon through the intermediate 1G4 level. The cross section of the transition from the ground to intermediate state (step 1) is the largest for a photon energy of about 1035 nm. The transition from 1G4 to 3P0,1 (step 2) occurs with the highest efficiency when pumping in the 840--860-nm interval. This combination of the required wavelengths can be reached in two ways. First, one can employ two pump waves with the corresponding wavelengths. The second approach makes use of the 850-nm pump only, but the core is additionally doped to convert the 850- to 1035-nm photons. For this purpose the Yb3+ ion is used. This arrangement is called avalanche pumping, because the first photon is absorbed here with a low efficiency, and the three subsequent ones, with a higher one.

There is a description of a Pr-doped ZBLAN (zirconium-barium-lanthanum-aluminum-sodium fluoride) up-conversion fiber laser [41]. Its excitation diagram required two pump waves, at 840 and 1020 nm, and a convenient two-wavelength source made of a 5-m long fiber 3.0 μm in diameter was developed for this application, which was chosen so as to yield the same amounts of unabsorbed pump power (840 nm) and laser radiation (1020 nm). This output radiation was employed to pump a Pr3+-doped ZBLAN up-conversion fiber laser which, when provided by mirrors for the blue, green, or red oscillation, produced 6.5 mW at 491 nm, 18 mW at 520 nm, and 55 mW at 635 nm, the total pump power being 380 mW at the above wavelengths.

Another wavelength of considerable device interest is 1140 nm. It is needed to pump efficient blue laser sources based on up-conversion in Tm3+-doped fluoride fibers. One obtained oscillation at 1140 nm in an Yb3+-doped fiber with gratings, with a diode-pumped Nd:YLF laser operating at 1047 nm used as a pump source. Next this 1140-nm source was employed to pump a Tm3+:ZBLAN up-conversion laser, which produced 30 mW of output power at a wavelength of 480 nm [42].

Andreas Tennermann with co-workers made use of the second pump diagram [43]. First they demonstrated emission at 635 and 520 nm obtained in Pr/Yb-codoped double-clad ZBLAN fibers pumped by a Ti-sapphire laser at 840 nm (see Laser Focus World, May 1998, p. 15). However the output radiation in the blue was weak and unstable. To produce lasing at 491 nm, one had not only to optimise the resonator but to use spectral selection for the blue line as well. The 491-nm emission of 150-mW output power remained stable for several hours. This result was achieved by Ti-sapphire laser pumping a single-clad fiber waveguide.

Further transition to cladding pumping (double-clad waveguide) should increase the output power. By using a Ti-sapphire laser emitting at 840 nm and mirrors for 491 nm, one obtained 165 mW for a 1.6-W pump power; the output power remained stable for several hours. When the pump power increased above 1.6 W, a line at 520 nm formed. Experiments were performed

with pumping by a laser diode operating at 840 nm and 140 mW power launched at 70% efficiency. In this case one obtained 14 mW at a wavelength of 491 nm.

The Photonics Cooperative Research Center reported an interesting development [44]. The researchers demonstrated a blue (492 nm) diode-pumped Pr-doped ZBLAN fluoride fiber laser. In this case the single-mode oscillation of two IR laser diodes emitting at 1017 and 835 nm was launched by a WDM element into the core. Each pump diode produced 50 mW of output power. The mirrors had a good reflectivity at 492 nm but a poor one for the red radiation. To increase the efficiency of the arrangement, the output mirror was made highly reflecting for the pump radiation. One obtained more than 1 mW at a wavelength of 492 nm.

Researchers from Stanford University have developed in the recent years a high-efficiency nonlinear optical material called PPLN (periodically poled lithium niobate). In contrast to conventional nonlinear crystals, where the interacting waves can be phase matched by the well known technique, in this material one makes use of quasi-phase matching (QPM). As a result of the nonlinear susceptibility being periodically modulated, the built-up phase mismatch vanishes after traversing the full period of this structure. In lithium niobate, this is done by periodically reversing its ferroelectric domain polarity when the phase mismatch reaches π [45]. PPLN is employed both in frequency doubling and optical parametric oscillator (OPO) arrangements to produce tunable emission in the IR range. Using quasi-phase-matched second harmonic generation in periodically poled lithium niobate (PPLN), Martin Fejer and researchers at Stanford University (Palo Alto, CA), collaborating with a group at IMRA America (Ann Arbor, MI), have generated 8.1 mW of frequency-doubled 777-nm output from a passively modelocked femtosecond erbium-fiber laser [46]. The system produced 190-fs, 90-pJ pulses, with conversion efficiencies as high as 25%.

The gain medium of the erbium-fiber soliton oscillator consisted of a 1-m-long fiber doped with 0.001% erbium; a large core diameter and high output coupling were used to keep circulating intensities low enough to minimize spurious nonlinear effects. A diode laser pumped the fiber laser with 150 mW at 980 nm to produce pulses with an average power of 50 mW and repetition rate of 88 MHz. This output was focused into a 1-mm-long, 0.5-mm-thick sample of PPLN, poled with 18.75-μm periods by an electric field; the crystal was maintained at 80°C to minimise photorefractive damage. Fiber laser SHG experiments with a 1-cm-long beta-barium borate crystal have achieved efficiencies of about 5%; the Stanford group says that a similar pump source with a 300-μm-long PPLN crystal would exceed 50% conversion efficiency. When combined with erbium-doped fiber amplifiers, frequency-doubled erbium-fiber lasers could provide an alternative to current solid-state ultrafast sources.

Second harmonic generation was achieved under CW and pulsed operation with a master oscillator and an Yb-doped fiber amplifier in combination with PPLN [47]. The PPLN sample was 20 mm long with a 0.5 mm $\times$ 5.0 mm aperture. It was prepared with grating period of 6.5 μm and was contained in a temperature-controlled oven to an accuracy of 0.10C. The crystal, which was uncoated at either the fundamental or harmonic, was normally configured for a fundamental wavelength of 1060 nm. A high power Yd-doped fiber amplifier was employed with a maximum saturated power of 7 W. The output of the fiber amplifier was fused coupled to a GRIN (GRadient INdex) lens providing collimation, and simple convex lens was used to focus into the PPLN crystal. In these experiments, seeding was exclusively provided by fiber-coupled semiconductor lasers. Under CW excitation at 1062 nm for an internal average power of 6W, 440 mW at 531 nm was obtained. The measured conversion efficiency was ~7%. Pulsed operation of the seeded system was readily obtained by modulating a 1064 nm seed diode to produce pulses of 2 ns (FWHM) over a wide range of selectable repetition rates and at

average output powers up to 7 W. A maximum conversion efficiency of 41% was recorded at peak power of ~25 W corresponding to an internal fundamental average power of 3.2 W and producing 1.3 W at 532 nm. In summary, authors have demonstrated high conversion efficiencies to the visible both in CW and pulsed formats through the application of seeded high power fiber amplifiers in combination with PPLN.

Authors [48] describe the first nanosecond PPLN OPO driven by a fiber laser. The source was frequency doubled by a PPLN sample before pumping a second, 20-mm-long, PPLN crystal. The OPO threshold was <10 μJ, with pump depletions of as much as 45% and a tunable signal range of 945-1450 nm (1690-4450-nm idler range).

At CLEO`98, researchers from Southampton reported two new fiber-laser-pumped optical parametric oscillators. P. E. Britton and others frequency-doubled Q-switched pulses from an erbium-fiber laser in PPLN, generating 70-microjoule pulses at 772 to 779 nm [49]. Those pulses pumped a PPLN OPO, which can be temperature tuned between 0.99 and 1.45 μm; researchers say this is the first singly resonant OPO pumped by a fiber laser. In a separate CLEO`98 paper, N. J. Traynor and others reported synchronously pumping a PPLN OPO with the amplified output of a ytterbium fiber laser operating at 1029 to 1060 nm, generating a signal beam tunable between 1.6 and 1.78 μm and an idler tunable between 2.5 and 3.14 μm [50].

An approach is proposed to developing compact laser sources to operate in the blue-green and UV ranges, which is based on third-harmonic generation (THG) in the near IR range in fiber waveguides [51]. It is essential that THG does not require the material to be anisotropic, so that in principle such a process can take place in a conventional waveguide as well. The first and third harmonics can be phase matched due to the fundamental and higher modes having different propagation constants. Finally, nonlinear frequency conversion of neodymium laser radiation (λ=1.06μm) was observed when this radiation was injected into the core of a single-mode optical fiber made of nitrogen-doped silica. This resulted in generation of visible violet and near-ultraviolet radiation (355-430 nm). The conversion efficiency was up to $2 \cdot 10^{-4}$. The observed UV radiation was the result of the following processes: generation of the third harmonic of the fundamental pump frequency, stimulated Raman scattering of the third harmonic, and generation of the third harmonics of the Raman-scattered components of the pump radiation. Lasing was also observed in the 380-430 nm wavelength range at colour centres associated with the presence of nitrogen in the silica core.

Main Processes and Mechanisms Restricting the Double-Clad Fiber-Laser Output Power

As stated above, the numerous available papers on fiber lasers contain many details of minor importance and only very scarce information on the fundamental limitations on output power and the parameters of the materials used. The most comprehensive paper dealing with the constraints of a fundamental character imposed on the output power of double-clad fiber lasers was published by Zenteno in 1993 [2]. Unfortunately, it considers the prospects only of neodymium-doped fiber lasers, and therefore the results it contains are not directly applicable to lasers of other types, in particular, of ytterbium-doped ones. However the processes and mechanisms limiting the output power of neodymium and ytterbium lasers are basically the same. Therefore, we are going to use the list of the above processes and mechanisms presented in [2]. Let us discuss briefly the part played by these processes and the possibility of making the corresponding estimates.

Propagation losses should become increasingly significant in fiber laser scale-up. Indeed, to increase the injected pump power, one has to increase the cross section of the inner cladding, which entails a decrease of the effective pump absorption coefficient; this should be compensated by increasing the fiber length. For this reason, we shall focus subsequently considerable attention on the propagation losses.

Parasitic oscillation, in our opinion, is not among fundamentally irremovable power constraints, because it takes place only in certain, not very well designed laser arrangements. Enhanced luminescence likewise cannot play anywhere near important role, because when operating in the lasing regime, the saturated gain achieved in the resonator length is by far not so high as the low-signal gain. The validity of this conclusion is borne out by experiment [54].

Of the thermal effects, the decrease of quantum efficiency with increasing temperature of the doped core appears to be the most serious factor [2]. When attempting scale-up by increasing the core diameter and, particularly, by replacing a single-mode core with a bundle of such fibers or a core of a larger diameter, the temperature at the center should increase together with the total heat dissipated. At the same time thermal stresses and lensing in the core are so small as to be hardly capable of playing a substantial role in scaling-up as well. Therefore we shall focus our attention primarily on a careful estimation of the core temperature.

Available information on the possibility of development of nonlinear effects is extremely contradictory; we shall present our relevant considerations later on. Finally, the optical strength of laser components is governed to a considerable extent by progress in the technology of their manufacture; we do not feel ourselves in position to make predictions in this area.

Waveguide Propagation Losses

We start with a brief discussion of the losses at the pump wavelength. Obviously enough, their existence simply reduces the pump efficiency in a ratio $\sigma_1/(\sigma_1+\sigma_2)$, where σ_1 and σ_2 (cm^{-1}) are, respectively, the useful and parasitic pump-absorption coefficients. For $\sigma_2 << \sigma_1$, these losses should not obviously affect the laser efficiency.

The problem of losses at the oscillation wavelength is less trivial. In principle, their existence sets an absolute bound on the power density of generated (or amplified) radiation. This limit is reached when the saturated gain coefficient becomes equal to the above losses. Because of the low propagation losses, this limit is extremely high; however approaching it closely entails a severe drop in the laser efficiency, because now nearly all of the pump power will be expended in loss compensation. In connection with this, we shall accept as allowable only such combinations of parameters for which the energy conversion efficiency in a laser resonator will not be too inferior to its theoretical limit. The corresponding estimates require carrying out an additional analysis.

The first account of a correctly made theoretical assessment of the laser conversion efficiency was given in [52]; identical calculations were soon published by Rigrod in [53], the paper referred mostly in the West. This problem was dealt with also in a number of subsequent papers. However in the vast majority of them the pump distribution along the length was assumed uniform, and the output mirror reflectivity, not too small. Besides, the analysis related mostly to the case of four-level media with the unpopulated lowest lasing level. Double-clad fiber lasers make use not only of four-level media (with neodymium serving as a sensitizer), but of three-level ones as well (with ytterbium). But the most essential point is here that the pump distribution along the fiber length is strongly non-uniform, and that the reflectivity of the output mirror is quite frequently on the order of one percent. This has forced us to perform the corresponding calculations. As for the pump distribution, we deemed it reasonable to compare four versions, more specifically, (a) the most widespread arrangement of the pump launched through the resonator mirror with 100% reflection of the lasing radiation, (b) the arrangement proposed in the preceding Report and based on pump injection from both ends of the fiber, (c) side pump launching [55], and (d) pumping from the output mirror side only.

Consider the case of a four-level medium with the unpopulated lowest operating level and homogeneous broadening of the lasing line. Here the population N of the upper operating level and the medium gain in intensity, k_g, are mutually proportional ($N = B k_g, B = \text{const}$). In the steady-state regime, we obtain for *N* the following balance equation

$$\frac{dN}{dt} = P - I k_g - B k_g/\tau = 0$$

where P is the number of replenishment events of the upper operating level per unit time per unit volume through pumping, I is the oscillation power density, and τ is the upper-level lifetime. Whence we obtain

$$k_g = \frac{k_g^0}{1+(\tau/B)I} \qquad (1)$$

where $k_g^0 \equiv \tau P/B$ is the gain coefficient at a given pump intensity in the absence of lasing radiation (i.e., for $I = 0$).

Neglecting interference between the lasing radiation propagating in the forward (relative to the output mirror with reflectivity R) and backward directions, we can write the following transport equations for the densities of these fluxes I_+ and I_-

$$\frac{dI_\pm}{dz} = \pm I_\pm (k_g - \sigma) \qquad (2)$$

where Z is the longitudinal axis ($0 \le z \le l$, l is the fiber length), and σ (cm^{-1}) is the propagation loss coefficient; these equations should be solved together with (1) and the boundary conditions $I_-(l) = R\, I_+(l)$, $I_+(0) = I_-(0)$.

We define the laser-power conversion efficiency in a resonator as the ratio X of the number of photons exiting the resonator to the total number of replenishment events N through pumping,

$$X = I_+(l)(1-R) \Big/ \int_0^l P(z)\,dz$$

Introducing dimensionless variables

$$x \equiv z/l, \quad \Sigma \equiv \sigma \cdot l, \quad u(z/l) \equiv I_+(z)\tau/B, \quad v(z/l) \equiv I_-(z)\tau/B, \quad k_g^0(z)l \equiv K(z/l)$$

we come to

$$\frac{du}{dx} = u\left(\frac{K}{1+u+v} - \Sigma\right), \quad \frac{dv}{dx} = -v\left(\frac{K}{1+u+v} - \Sigma\right) \qquad (3)$$

having found from this system of nonlinear differential equations $u(x)$ and $v(x)$ for given $K(x)$, Σ, and the boundary conditions $u(0) = v(0)$, $v(1) = R\,u(1)$, one can readily calculate the efficiency from the relation

$$X = \frac{(B/\tau)\,u(1)(1-R)}{\int_0^l (B/\tau)\,k_g^0(z)\,dz} = (1-R)\,u(1)/Q,$$

where $Q \equiv \int_0^1 K(x)\,dx$.

We shall be able to see later on, that Q and Σ are the most important parameters, which govern the character of the solution; therefore it appears appropriate to explain their meaning. The quantity Q determines the small-signal gain coefficient over the fiber length in the absence of losses ($\Sigma = 0$), which is e^Q. The quantity Σ, in its turn, accounts for the attenuation of the same signal, whose intensity decreases e^Σ times over the fiber length in the absence of amplification (i.e., for $Q = 0$).

We wrote a program to solve (3) which is faster when standard and performed calculations over the broadest possible range of parameter variation. The subsequent data will refer to the case where the fiber length and the effective pump absorption coefficient are such that the inverse population and the small-signal gain coefficient k_g^0 decrease 100 times over the fiber length, so that the pump radiation is used to 99%. Then the above four versions of pump launching can be identified with K(x) distributions of the type $M\cdot 10^{-2x}$, $M\left(10^{-2x}+0.01\cdot 10^{2x}\right)$, $M\left(10^{-2|x-0.5|}+0.01\cdot 10^{2|x-0.5|}\right)$ and $M\cdot 0.01\cdot 10^{2x}$, to which, in their turn, correspond the values of Q of $0.215M$, $0.43M$, $0.43M$ and $0.215M$. Recall that the first version is pump launching from a resonator mirror opaque for the lasing radiation (x = 0), and the second, double-sided injection (the pump intensities from both fiber ends are assumed equal). In the third version, the pump is launched midway (x = 0.5); its fluxes launched in opposite directions are equal, with only one tenth of them reaching the resonator mirrors, and it is this fraction that gets reflected from the latter back to the fiber midpoint. Finally, in the fourth arrangement the pumping is done from the resonator output-mirror side only.

In trying to generalize the relations found in the course of the numerical calculations, we discovered quite unexpectedly that in the case of comparatively low losses these relations can be fitted perfectly over a very broad range of parameter variation by the simplest expressions from [2, 3], provided the gain coefficient k_g^0, which was employed there and assumed constant, is replaced by its length-averaged value. Recall that these expressions predicted an optimum reflectivity R_{opt} of the resonator output mirror and the corresponding efficiency X_{max} reached under these conditions:

$$\ln\left(1/R_{opt}\right)=2\sigma\left(\sqrt{k_g^0/\sigma}-1\right),\quad X_{max}=\left(1-\sqrt{\sigma/k_g^0}\right)^2.$$

After this replacement and transfer to our notation, the expressions take on the form

$$\ln\left(1/R_{opt}\right)=2\Sigma\left(\sqrt{Q/\Sigma}-1\right),\qquad X_{max}=\left(1-\sqrt{\Sigma/Q}\right)^2. \tag{4}$$

Consider an example. Figure 1 displays the results of numerical calculations made for $M=5$ and $\Sigma=0.2$. Curve 1 corresponds to the first and the fourth versions of pump injection (one-sided, $Q=1.075$), for which the data are practically the same, 2 - to the second and third arrangements ($Q=2.15$).

At the same time relations (4) yield here for the first arrangement $R_{opt}==0.590$ and $X_{max}==0.323$, and for the second and third versions, $R_{opt}=0.402$ and $X_{max}=0.483$. The differences from the values of the corresponding parameters in the figure are negligibly small.

It appears significant that the energy conversion efficiency reached under optimum R in the second and third pumping arrangements is substantially higher than that in the first. There is nothing strange in it, because, for equal M, the mean pump intensity, which is proportional to Q, and, hence, the pump intensity in excess of the lasing threshold reached in one-sided injection is one half that obtained in the other two launching arrangements. This means that the double-sided energy injection proposed in the preceding Report provides a more than twofold increase in output power (because not only the pump power is doubled but the efficiency is increased). In this particular example, the total gain in power turns out to be threefold.

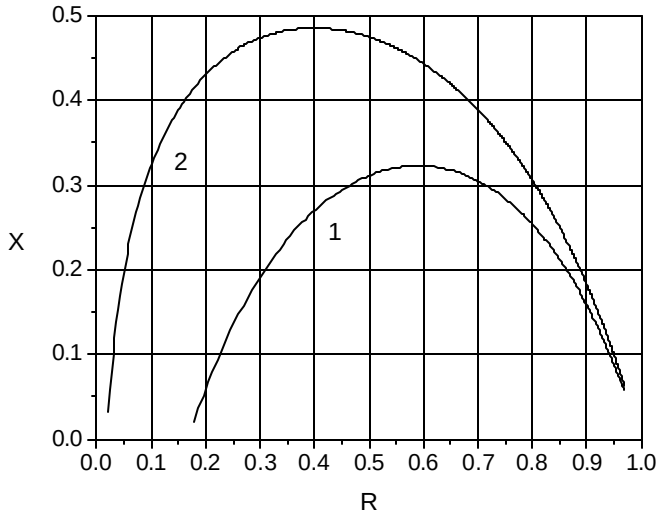

Figure 1

Some results of the numerical calculations are presented in Tables 1--4, which relate to the above four pumping geometries. They list the energy conversion efficiencies X_{max} for given Σ and Q/Σ reached at the values of R which are optimal for each parameter combination and not specified here. The ratio Q/Σ was chosen as a key parameter not only because it has the meaning of the pump intensity in excess of the lasing threshold in the case of a resonator made up of totally reflecting mirrors, and, as such, enters equations (4). It appears more significant for us here that in the absence of pump absorption in the inner cladding material, this ratio is preserved also in scale-up achieved by increasing the cross sectional area of this cladding.

Indeed, let this area be increased N times; the launched pump power can also be increased by the same factor. Under these conditions, the pump density injected into the fiber and, accordingly, the gain coefficient will not change. Because the effective pump absorption coefficient decreases proportional to the core/inner-cladding area ratio, i.e., by the same factor N, we may conclude that in order for the fraction of the total pump radiation absorbed in the fiber to remain unchanged, the fiber length has to be increased N times. We readily see that the shape of the pump distribution along the fiber remains the same and, hence, the integrated gain coefficient Q increases by the same factor N as Σ.

It thus follows that by moving down a column in a Table one can directly predict the result of a scale-up for the given initial parameters and the pump geometry.

The top row in the tables (Σ = 0.001) corresponds to the case of very small lengths (or low losses). The figures here are in complete agreement with equations (4) for all the four pumping geometries. Examining the other rows, it is evident that as Q/Σ increases, X_{max} tends to certain limits whose values fall off droningly with increasing losses.

Table 1. Pump launching from a resonator mirror opaque for the lasing radiation

Σ	Q/Σ						
	6	12	25	50	100	200	∞
0.001	0.350	0.506	0.640	0.736	0.809	0.862	0.999
0.2	0.347	0.497	0.622	0.707	0.765	0.802	0.855
0.3	0.341	0.486	0.601	0.675	0.723	0.752	0.790
0.6	0.315	0.433	0.516	0.564	0.591	0.607	0.626
1	0.268	0.350	0.402	0.429	0.444	0.453	0.462
2	0.155	0.187	0.205	0.214	0.219	0.221	0.224
4	0.048	0.056	0.060	0.062	0.063	0.063	0.064

Table 2. Double-sided pumping

Σ	Q/Σ						
	6	12	25	50	100	200	∞
0.001	0.350	0.506	0.640	0.737	0.810	0.863	1.000
0.2	0.350	0.506	0.640	0.735	0.802	0.846	0.907
0.3	0.350	0.506	0.638	0.727	0.785	0.820	0.865
0.6	0.350	0.501	0.613	0.677	0.713	0.733	0.757
1	0.347	0.475	0.556	0.597	0..619	0.631	0.644
2	0.312	0.387	0.426	0.444	0.454	0.458	0.463
4	0.235	0.270	0.287	0.294	0.298	0.300	0.302

Table 3.The pump is launched midway

Σ	Q/Σ						
	6	12	25	50	100	200	∞
0.001	0.350	0.506	0.640	0.737	0.810	0.863	1.000
0.2	0.349	0.504	0.637	0.730	0.797	0.840	0.905
0.3	0.349	0.503	0.631	0.719	0.778	0.814	0.862
0.6	0.345	0.489	0.598	0.663	0.700	0.722	0.747
1	0.332	0.452	0.532	0.573	0.596	0.608	0.622
2	0.273	0.338	0.373	0.390	0.398	0.402	0.407
4	0.160	0.181	0.191	0.196	0.198	0.199	0.200

Table 4. The pumping is done from the resonator output-mirror side only.

Σ	Q/Σ						
	6	12	25	50	100	200	∞
0.001	0.350	0.506	0.640	0.737	0.810	0.863	1.000
0.2	0.350	0.509	0.648	0.751	0.827	0.880	0.959
0.3	0.353	0.515	0.658	0.762	0.834	0.879	0.940
0.6	0.363	0.537	0.682	0.771	0.824	0.853	0.887
1	0.383	0.561	0.685	0.751	0.787	0.805	0.826
2	0.422	0.563	0.637	0.670	0.686	0.695	0.702
4	0.416	0.486	0.516	0.529	0.534	0.537	0.540

As Σ increases, the energy conversion efficiency decreases droningly. The only exclusion to this rule is the fourth pumping arrangement, where scale-up is capable of even increasing

substantially the energy conversion efficiency at small Q/Σ ratios. However this case would hardly be of any interest, because the absolute values of the efficiency here are low.

The high energy conversion efficiency observed experimentally evidences that the attainable values of the Q/Σ ratio are fairly high; therefore the last columns of the tables are of particular interest. Examining them, we can see that the most favorable for a scale-up are the second and fourth pump versions, where the pump is launched either from both sides of the fiber or from the output resonator mirror. If efficiency losses of the order of 10% are considered acceptable, the value of Σ can be raised under double-sided pumping to about 0.3, and when pumped only from the output mirror, to unity. However when comparing the second with the fourth arrangements, one should not overlook the fact that, for identical pump sources, the Q/Σ ratio in the second arrangement is twice higher, and therefore it is with this setup that one can attain the maximum possible output power.

In conclusion to this Section, we shall dwell briefly on the three-level media employed in ytterbium-doped lasers. We have carried out the corresponding calculations for this case too, however the results obtained do not have the same degree of universality. The reasons for this lie in that even in the case of homogeneous line broadening one has here an additional parameter, namely, one has to know, besides the coefficient of proportionality B relating the inverse population to the gain coefficient, the fraction of the total number of the sensitizer atoms which is involved in this inverse population. Also, the pump absorption coefficient in the core is no longer constant and begins to depend on the inverse population, which, in its turn, is a function not only of the pump power but of the lasing radiation density as well. Suffice it to say that the main qualitative relations are here the same. The largest energy conversion coefficients are achieved when pumping from the side of the output resonator mirror, and the highest power, under double-sided pump launching.

Thermal Effects

All possible consequences of heat dissipation in a fiber were comprehensively analyzed in [2]. It was found that because of the extremely small single-mode core diameter the only factor capable of seriously degrading the lasing power is the increasing temperature of the core, which is accompanied by a decrease of the quantum luminescence efficiency. The only point in [2] that raised our doubt was the use of a calculational model in which the rectangular cross section of the inner cladding was replaced by a circular one of the same area. The fact is that the heat conductivity coefficient of the outer-cladding material is many times smaller than that of the inner one, and therefore it is the outer cladding that should suffer from the main temperature drop, which is determined primarily by its thickness. At the same time two of the boundaries of a rectangular inner-cladding cross section pass relatively closely to the outer boundary of the outer cladding. It thus appears that the conditions of heat removal here are more favorable than in the case of the inner cladding having a circular cross section of the same area. These considerations permit a qualitative conclusion that the model employed in [2] yields an overestimate for the total temperature drop; realistic data required carrying out numerical calculations, which we did.

Because forced cooling of a fiber is easy to provide (for instance, by an air flow), we considered the temperature of its outer surface given and set it, for the sake of simplicity, to zero. Thus the temperatures quoted in what follows are actually the differences between the local temperatures and that of the outer surface. Finally, the dissipated heat was assumed to be concentrated in the core, and the parasitic absorption of the pump radiation in the inner cladding was neglected (as it was in the calculations presented in the preceding Section), which is allowable when estimating the extreme characteristics.

The calculations were carried out in dimensionless units assuming the following relation between the conventional, T, and dimensionless, t, temperatures:

$$T = t \cdot \frac{w r_1^2}{k_3} \tag{5}$$

where w is the heat dissipation power per unit core volume, r_1 is the core radius, and k_3 is the heat conductivity coefficient of the outer cladding material. Because the heat power dissipated per unit fiber-core length is $P_0 = w \cdot (\pi \cdot r_1^2)$, we obtain

$$T(0) = t(0) \cdot \frac{P_0}{\pi \cdot r_1^2} \frac{r_1^2}{k_3} = \frac{t(0)}{\pi \cdot k_3} \cdot P_0 \equiv \alpha \cdot P_0 \tag{6}$$

where α is a coefficient of proportionality relating the total temperature drop (from the core center to the waveguide edge) to the power dissipated per unit core length.

This coefficient depends on the waveguide geometry and the heat conductivity coefficients of the quartz glass, k_1, and of the outer cladding, k_3. Presented below are data for three inner-cladding configurations. For the rectangular cross section we chose the typical dimensions quoted in [2], namely, 300 x 80 μm^2; temperature distributions for a square and a circular cross section of the same area were also calculated. In the latter case of cylindrical geometry for the inner cladding with a radius r_2, the steady-state heat transport problem is readily solved to yield the following expression for the α coefficient:

$$\alpha = \frac{1}{4\pi \cdot k_1}\left[1 - 2 \cdot \left(\ln\left(\frac{r_1}{r_2}\right) + \frac{k_1}{k_3} \cdot \ln\left(\frac{r_2}{r_3}\right)\right)\right] \qquad (7)$$

which, for the dimensions $r_2 = 8.74 \cdot 10^{-3}$ cm, $r_1 = 3.5 \cdot 10^{-4}$ cm, and $r_3 = 2.0 \cdot 10^{-2}$ cm, yields $\alpha \approx 2.00 \frac{m \cdot {}^0 K}{W}$.

For the square cross section of the outer cladding (155 x 155 μm^2), this coefficient has practically the same magnitude. Finally, for the waveguide with a rectangular cross section we obtain $\alpha \approx 1.75 \frac{m \cdot K}{W}$. Thus the temperature drop is here indeed smaller than the one calculated with the model of [2]. However the difference is even less than 15%, and therefore the figures quoted in [2] may be used for rough estimates of the limiting possibilities of fiber lasers.

The calculation of the α coefficients required carrying out cumbersome numerical computations of the temperature fields. The results obtained are presented below in the form of both 3D plots and the corresponding contour maps.

Circle

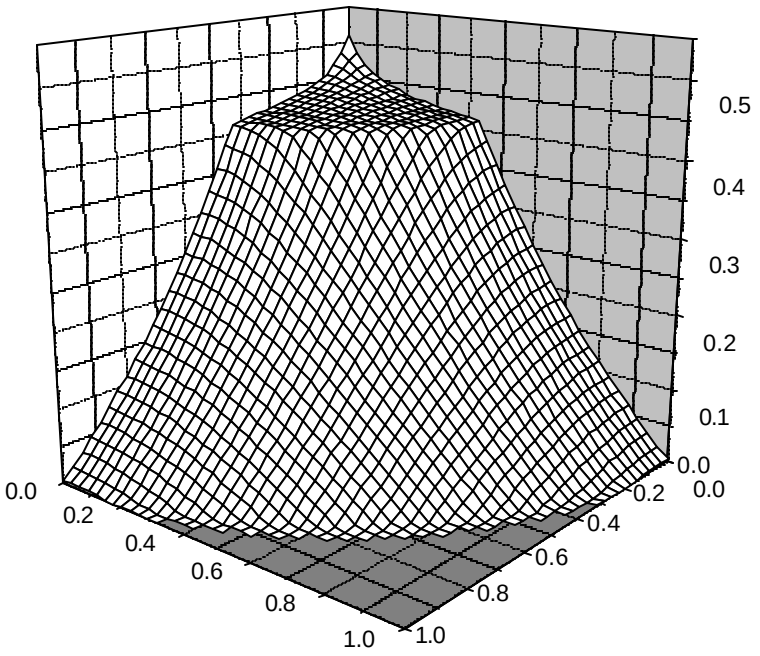
0.5
0.4
0.3
0.2
0.1
0.0
0.0
0.2
0.4
0.6
0.8
1.0
0.0
0.2
0.4
0.6
0.8
1.0

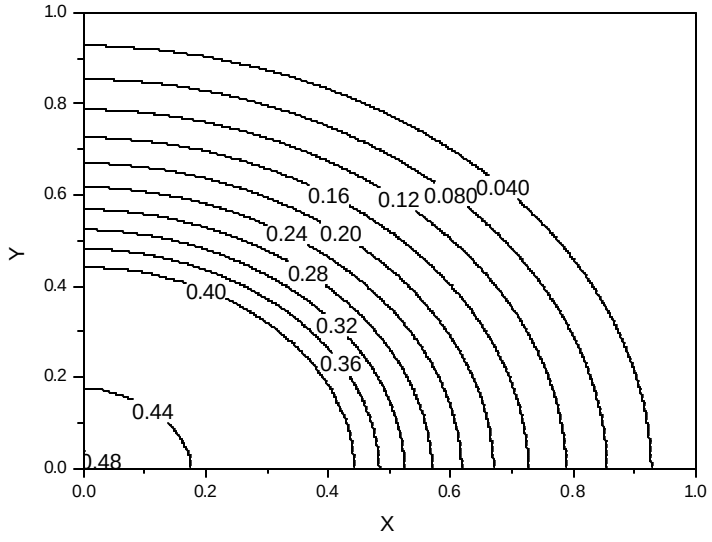
1.0
0.8
0.6
0.4
0.2
0.0
Y
0.0
0.2
0.4
0.6
0.8
1.0
X
0.040
0.080
0.12
0.16
0.20
0.24
0.28
0.32
0.36
0.40
0.44
0.48

Square

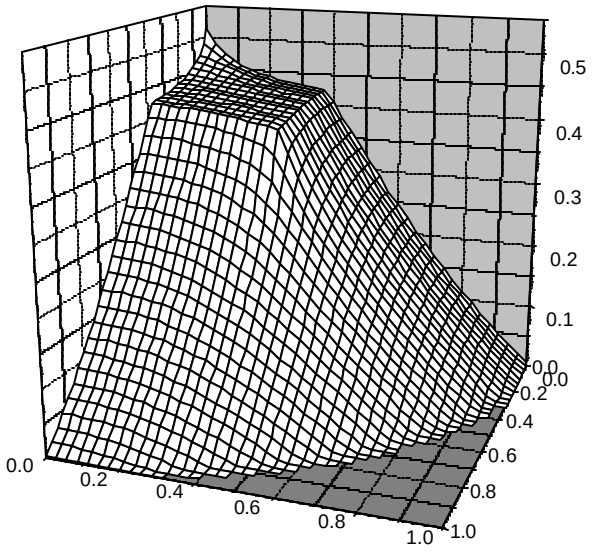
0.5
0.4
0.3
0.2
0.1
0.0
0.0
0.2
0.4
0.6
0.8
1.0
0.0
0.2
0.4
0.6
0.8
1.0

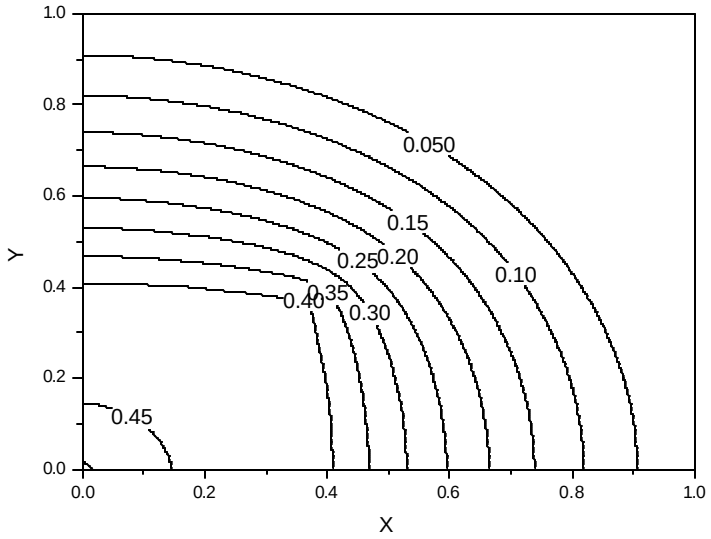
1.0
0.8
0.6
0.4
0.2
0.0
Y
0.0
0.2
0.4
0.6
0.8
1.0
X
0.050
0.10
0.15
0.20
0.25
0.30
0.35
0.40
0.45

Rectangle

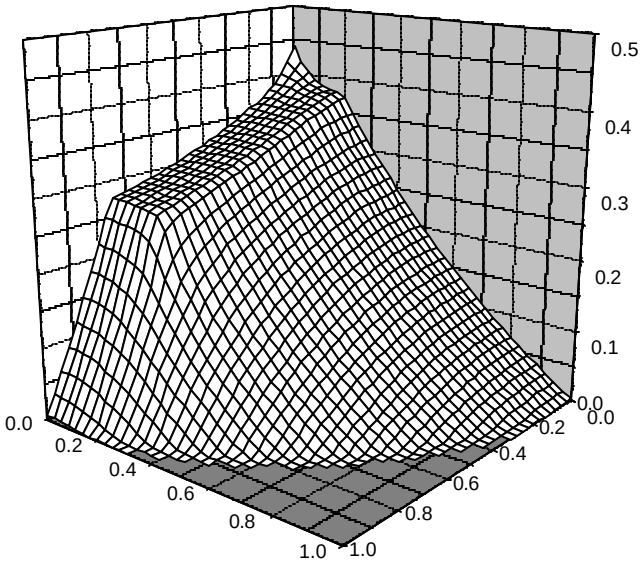
0.5
0.4
0.3
0.2
0.1
0.0
0.0
0.2
0.4
0.6
0.8
1.0
0.0
0.2
0.4
0.6
0.8
1.0

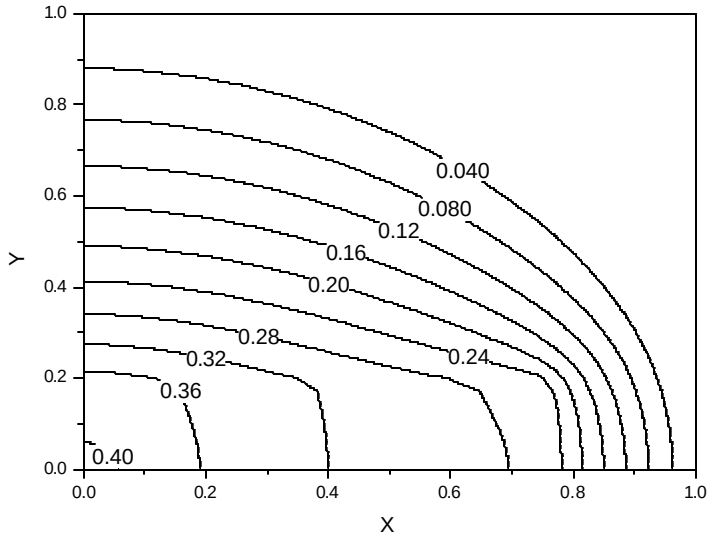
1.0
0.8
0.6
0.4
0.2
0.0
Y
0.0
0.2
0.4
0.6
0.8
1.0
X
0.040
0.080
0.12
0.16
0.20
0.24
0.28
0.32
0.36
0.40

Nonlinear Effects

As a rule, the nonlinear optical effects appearing spontaneously in laser systems are deleterious and degrade the operation of the system in one way or another. Therefore one should have at least approximate estimates of the threshold conditions at which these effects may become manifest.

The nonlinear optical effects, which may set in in fiber lasers, can be divided in two classes:

(i) Effects depending on the average power. In our case, these are thermal phenomena (thermal lensing, which may be accompanied by thermal self-focusing);

(ii) Effects depending on the peak laser-pulse power. The nature of these phenomena is more diverse (self-focusing caused by the Kerr nonlinearity, SBS, SRS, four-wave mixing, phase self-modulation which may give rise to pulse compression, and a number of other effects).

The change in the refractive index caused by the Kerr nonlinearity can be written for the case of wave propagation in a waveguide as

$$\Delta n_{NL} = \frac{n_2 \cdot P}{A_{eff}} \qquad (8)$$

This relation follows from the general expression for induced nonlinearity, in which the light intensity is replaced by the ratio of the wave power P to the effective cross-sectional area of the waveguide core Aeff.

The critical power at which self-focusing sets in can be roughly estimated from a relation following directly from [56]. It is maintained that beam self-focusing occurs when the induced nonlinearity reaches the level

$$\Delta n_{NL} \approx \frac{\lambda^2}{2n\pi A_{eff}}$$

Thus self-focusing effects may be expected to appear at a critical power

$$P_c \sim \frac{\lambda^2}{2\pi n n_2} \ . \qquad (9)$$

For fused quartz, n2 ≈ 3×10^{-16} cm^2/W, so that Pc ≈ 4 MW. Such a large value of critical power provides assurance that this effect will not manifest itself in the scaling-up of fiber lasers.

When describing SBS and SRS effects in an optical fiber, the growth of the scattered wave intensity in a distance dz is given by

$$I(z+dz) = I(z) \cdot \exp\left(g \cdot \frac{P}{A_{eff}} \cdot dz \right)$$

where g is the gain coefficient, and the other quantities have been defined earlier. As follows from this expression, the role of stimulated scattering processes increases with increasing length of the part of the waveguide in which the scattered wave forms. This dependence arises naturally from the effect of accumulation, which is accounted for by the coherent contributions of each part of the waveguide in this effective length L_{eff}.

We shall dwell now briefly on the Brillouin and Raman gain effects. The gain coefficient for the SBS $g_B \approx 4\times10^{-9}$ cm/W. The Raman gain coefficient $g_R \approx 4\times10^{-11}$ cm/W, i.e., it is substantially smaller. A comparison of these gain coefficients seems to suggest that in order to obtain the same scattered power with SRS, one would have to have a considerably higher signal-wave power. In particular, the same conclusion is drawn in [57]. One should, however, bear in mind that the Brillouin amplification is characterized by an extremely narrow linewidth. Therefore another above-mentioned author [2] maintains that SBS should be inefficient in high-power fiber lasers with broad gain linewidths. We would like to add that using SBS gain coefficients obtained in experiments with bulk lasers may turn out to be inapplicable to single-mode fibers. In this case, the diffraction of an acoustic wave may affect substantially the formation of the latter. Indeed, the dimensions of the waveguide core exceed by only an order of magnitude the acoustic wavelength, and the wave is quickly dissipated by diffraction. Obviously enough, this factor will result in a decrease of the SBS gain.

In contrast to SBS, Raman gain in fibers is characterized by a large linewidth. The critical signal-wave power for SRS is obtained from the expression employed usually when estimating the stimulated scattering threshold:

$$g_R P_c L_{eff} / A_{eff} = 16 . \qquad (10)$$

Accepting 10 m for the characteristic waveguide length, this yields for a single-mode fiber with a 7-μm-dia. core Pc ≈ 500 W. It should be taken into account that the effective length increases for a waveguide placed in a high-Q resonator. Besides, the above expression provides only a rough estimate and is not capable of giving an idea of the scattered power obtained. However this estimate suggests that in the course of scaling-up one may observe uncontrollable stimulated Raman scattering.

Possible Causes **of Fiber Heating**

In this Section, we are going to consider briefly the effects, which cause fiber heating. We shall assume the laser to operate in the CW mode.

As stated above, the only factor capable of seriously reducing the generated power in a single-mode fiber is the decrease of the quantum luminescence efficiency with increasing temperature of the fiber core. In principle, heat can be released in fiber lasers in several processes. First, this is the difference between the pump and oscillation photon energies in nonradiative transitions from the absorption band to the upper lasing level. If only this process operated, the fraction of the power converted to heat would obviously be

$$1-\frac{\lambda_p}{\lambda} \tag{11}$$

Here λ_p is the wavelength of the pump radiation, and λ is the lasing wavelength. With the pumping done at 970 nm and Yb radiating at 1030 nm, about 6% of the pump energy would be converted to heat. Second, the quantum efficiency of the lasing transition ϕ is less than λ_p/λ because of the existence of nonradiative transitions from the upper to the lower lasing level. Finally, stimulated Raman scattering in the fiber can also produce heat. This process converts to heat up to 5% of the photon energy in each stimulated scattering event. Thus, in principle, this mechanism of heat dissipation could compete with the first one for a strong enough scattering. Note that heat is dissipated in SRS not only in fiber lasers but in an undoped fiber as well, provided the transmitted power is high enough. Thus, it is this process that can dominate power transport along an optical fiber. Let us estimate the power of a wave propagating in an optical fiber, at which Raman scattering may contribute noticeably to fiber heating.

The Section dealing with SRS presented an estimate of the wave power, which may give rise to strong scattering in a single-mode fiber with a core diameter of a few microns. This estimation yielded a few hundred watts for the power. We want to estimate the wave power at which the above scattering would result in the maximum allowable fiber heating. Let us make an approximate estimate of this critical wave power for the steady-state case, which corresponds to the free-running lasing of the fiber laser operation.

Introduce the following notation of the quantities to be used. Let the intensity of the wave formed in the oscillation is I, and its frequency ν. Stimulated Raman scattering generates a Stokes scattered-light component of intensity IS shifted by an amount $\Delta\nu$. Neglecting linear absorption in our estimation, the scattering process will be described by the following equations

$$\frac{dI}{dz} = -g \cdot I \cdot I_s \cdot \frac{\nu}{\nu_S} \tag{12}$$

$$\frac{dI_S}{dz} = g \cdot I \cdot I_S \tag{13}$$

Here g is the Raman gain coefficient.

Obviously enough, the heat power dissipated in a volume of length Δz and unit cross sectional area can be written as

$$w \cdot \Delta z = \left[I(z) - I(z+\Delta z)\right] - \left[I_s(z+\Delta z) - I_s(z)\right] = \left(-\frac{dI}{dz} - \frac{dI_s}{dz}\right) \cdot \Delta z$$

where w is the heat power density. Combining this equation with the two preceding equations (12) and (13), we obtain

$$w = g \cdot I \cdot I_S \cdot \frac{\Delta\nu}{\nu} \qquad (14)$$

where $\Delta\nu = \nu - \nu_S$.

To make a rough estimate of the maximum possible dissipated heat power, we assume the total intensities of the signal and scattered waves to be constant along the fiber length:

$$I + I_S = I_0$$

The heat release reaches a maximum obviously when the signal and scattered waves have equal intensities:

$$w_{max} = \frac{g \cdot \Delta\nu \cdot I_0^2}{4\nu}$$

We can now use the expressions derived in the second part of the Report, which relate the temperature at fiber core centre, T(0), with the dissipated heat power per unit length of the fiber, P_0. It was assumed that the fiber surface is at zero temperature:

$$T(0) = \alpha \cdot P_0 \qquad (15)$$

where α is a coefficient of proportionality. This coefficient depends on the fiber geometry and the thermal conductivity coefficients of the fiber materials. For instance, for the case of circular geometry with an inner cladding of radius r_1 and an outer (second) cladding of radius r_2, the expression for the α coefficient has the form

$$\alpha = \frac{1}{4\pi \cdot k}\left[1 - 2 \cdot \left(\ln\left(\frac{r_C}{r_1}\right) + \frac{k}{k_2} \cdot \ln\left(\frac{r_1}{r_2}\right)\right)\right]$$

where k and k_2 are the thermal conductivity coefficients of the quartz glass and of the outer cladding, respectively, and rc is the radius of the Yb-doped core. Using the dimensions of the single-mode double-clad fiber specified in the preceding Section, one obtained

$$\alpha \approx 2.00 \frac{m \cdot {}^0K}{W}$$

Thus, combining the above expressions yields

$$T(0) = \frac{g \cdot \Delta\nu \cdot I_0^2}{\nu} \frac{\alpha \cdot \pi r_1^2}{4}$$

Assuming a critical temperature $T_?$ at which SRS processes may bring about a substantial heating of the fiber, the expression for the corresponding critical light intensity takes on the form

$$I_C = \sqrt{\frac{4}{\alpha \cdot \pi r_1^2} \cdot \frac{T_C \cdot \nu}{g \cdot \Delta\nu}} \qquad (16)$$

and the corresponding critical power can be derived from the relation

$$P_c = \pi r_1^2 \cdot I_C = \sqrt{\frac{4\pi r_1^2}{\alpha} \cdot \frac{T_C \cdot \nu}{g \cdot \Delta\nu}} \qquad (17)$$

The value of $T_?$ is determined from the relation approximating the drop of the quantum efficiency ϕ with increasing temperature. This relation originates, in its turn, primarily from the temperature dependence of the nonradiative decay rate of the upper lasing level. This decay may proceed in different ways, which quite frequently are difficult to describe analytically. In the case of Yb-doped fused quartz of interest to us here, among the processes contributing to the decay of the upper lasing level are the multi-photon transitions, concentration quenching of the luminescence, diffusion and cross-relaxation of excitation. The critical temperature was estimated for the case of Nd-doped core [2]. The difficulties involved in taking into account all the above processes and their contribution to the upper-level decay rate require correcting the calculations in accordance with experimental data. The author [2] comes to the conclusion that at a core temperature of ~100^{0}C the laser quantum efficiency drops by 6%. We do not have such data for the Yb-doped fiber, and therefore accept the same value Tc ~100^{0}C in our estimates. The Raman gain coefficient for the neodymium laser radiation presented in our preceding Report is $g \sim 10^{-11}$ cm/W, and the Stokes frequency shift is $\Delta\nu$ = 440 cm^{-1}.

Accepting the fiber core dimensions and the calculated coefficient α for the cylindrical shape of the inner cladding used in the preceding Section, Eq. (17) yields about one hundred kW for the critical wave power in the core. Such a power just cannot be reached in the single-mode fiber lasers considered here. Thus the above estimate permits one, when analyzing the reasons constraining the output power of single-mode fiber lasers, to neglect the mechanism of luminescence quenching associated with heat dissipation through stimulated Raman scattering.

We can now estimate the power, which can be extracted from unit core length assuming nonradiative transitions of excited atoms from the absorption band to the upper lasing level to be the only fiber heating mechanism. We shall assume the fraction of the power dissipated as heat to be determined only by the quantum efficiency of the laser transition. Then the laser power P extracted from unit length of the fiber will be related to the heat power dissipated in the core through

$$P_0' \approx \frac{\lambda - \lambda_p}{\lambda_p} \cdot P$$

We use again Eq. (15), with $T_C \sim 100^0$C taken as the critical temperature. We obtain the following expression to estimate the critical power at which the fiber is heated to the critical temperature:

$$P_C = \frac{\lambda_p}{\lambda - \lambda_p} \cdot \frac{T_C}{\alpha}$$

For λ_P = 970 nm and λ = 1030 nm, this yields the following estimate for the critical laser power per meter of a single-mode fiber

$$P_C \approx 800 \frac{W}{m} \qquad (18)$$

Note that although this estimate of the critical power was obtained for a fiber with specific dimensions of the core and of the claddings, its dependence on the core size is fairly weak within a broad range. For instance, an increase of the core diameter from $3.5\ 10^{-4}$ cm to 10^{-3} cm (i.e., by three times) changes the α coefficient by ≈5%. This follows from the fact that the temperature drop occurs primarily in the second (outer) cladding. Hence, the estimate of the critical power varies very little with increasing core diameter. It should be stressed that this estimate is based on the assumption that the critical temperature obtained for an Yb-doped fiber differs little from that for a Nd-doped one.

Obviously enough, the crucial point in designing a laser is the correct choice of the fiber cooling system. For instance, the limiting power level given by (18) assumes that the cooling system is capable of removing heat power of about 50 W from one meter of the fiber. This figure is obtained for the above efficiency of 6% for the Yb-doped fiber. The area of the surface in contact with the external reservoir is in our case approximately 10 cm^2. Thus, the cooling system should provide heat removal of ≈ 5 W/cm^2. The dominant factor to be taken into account in designing the cooling system is evidently the surface thermal conductivity coefficient h. Its determination being connected with a number of problems, we shall neglect this and limit ourselves rather to taking an order-of-magnitude estimate of h for various cooling mechanisms. For instance, in the case of free convection in air, h ~ 0.01 W/(cm^2 deg). It appears fairly clear that this cooling mechanism cannot in principle provide removal of the above heat flux from the fiber. Reasonable values of the heat flux removed by free convection in air can probably be obtained at temperature drops of the order of 20o, which yields a critical laser power per meter of a single-mode fiber 25 times lower than given by (13). In other words, this cooling mechanism is not capable of providing removal of more that 10÷30 W per meter of a single-mode fiber. Experiment shows that the surface thermal conductivity coefficient under liquid cooling can be approximately a thousandfold higher than that for the air cooling. It might seem that this cooling mechanism could ensure heat removal figures given in (18). However, our previous consideration disregarded the limiting pump power that can be efficiently absorbed by the fiber core. It is this factor that may be crucial in an attempt at reaching the maximum possible power for a given fiber configuration.

Limitations Caused by the Maximum Pump Power Absorbed by the Core

The problem of the maximum pump power absorbed by the core is considered in [2]. One can find there an expression for the maximum pump power per unit length Pmax that can be efficiently absorbed in a fiber laser. This quantity can be derived from the saturated pump power Psat.pump per absorption length La. The expressions for the latter two parameters can be derived from the relations [58]

$$P_{sat,pump} = (h\nu_p / \sigma\tau_{f,0}) \cdot (A/G) \quad \text{and} \quad \sigma N G L_a = 1$$

Here $h\nu_p$ is the pump photon energy, σ is the absorption cross section, A is the core area, $\tau_{f,0}$ is the fluorescence decay time at room temperature, N is the rare-earth ion concentration, and the geometric factor G takes into account the pump beam cross section, so that $G \approx 1$ for a simple fiber laser, and $G = (r_C/r_1)^2$ for a double-clad laser. Thus

$$P_{max} = \frac{P_{max,\,pump}}{L_a} = \frac{h\nu_p \cdot A \cdot N}{\tau_{f,0}} \qquad (19)$$

Taking, for definiteness, a Nd-doped fiber, we obtain a typical ion concentration $N = 2 \cdot 10^{25}$ ion·m^{-3}, $h\nu_p = 2.46\ 10^{-19}$ J, and $\tau_{f,0} = 400$ μs. For a core radius of single-mode fiber rc = 3.5 μm used in the preceding Section, this yields $P_{max} = 0.5$ W/m. The author maintains that using Yb for a dopant one can reach an order-of-magnitude higher concentration of active ions. However, because $\tau_{f,0} = 2$ ms [59], we obtain P_{max} of the same order of magnitude. Obviously enough, the higher P_{max}, the higher should be the output power of a fiber laser. These estimates permit a conclusion that it is the maximum absorbed pump power that is a factor constraining the fiber laser power.

Recall that the above consideration has dealt with the CW operation of the laser. As for pulsed systems, the nonlinear processes considered in the preceding Report should become, depending on the actual laser parameters, most likely the major limiting factor.

Possible Ways of High-Power Scaling

The limiting specific pump power

$$\frac{P_{max}}{A} = \frac{h\nu_p \cdot N}{\tau_{f,0}} \qquad (20)$$

determines the maximum possible specific power that can be extracted in a laser system. As seen from this expression, the only way to increase this parameter lies in developing a technology to raise the rare-earth ion concentration in the fiber core. To boost the laser output power, one can also increase the gain medium volume by increasing either (i) the fiber length or (ii) its cross sectional area.

(i) When increasing the fiber length, two factors should be borne in mind. First, in trying to take the maximum possible length we immediately meet with the constraint associated with propagation losses. The laser efficiency is primarily affected by the pump wave losses. Second, in order for the pump power absorbed by the core over a large fiber length to be close to its limiting value (20), the wave end-launched into the inner cladding should have a high average power. The currently reached radiation strength of fibers is a few kW per square mm, and it is not a factor limiting the use of high pump levels. In this case, the constraint will be most likely imposed by the insufficient brightness of the laser diode arrays. The current record-high pump-power density levels are of the order of $0.7 \div 1$ kW/mm^2. Thus, in order to increase the pump level of a fiber, one has to increase its diameter. However, increasing the cladding diameter while maintaining the core diameter constant does not improve proportionally the core pumping. If the pump radiation is distributed uniformly over the fiber cross section (this is exactly the case because of the multi-mode nature of the pump), the pump power launched into the core is determined by the G factor [60]. Thus, we come to the conclusion that one has to increase the core diameter.

(ii) Increasing the core cross sectional area can be attained by either using a fiber with many active single-mode cores or by employing a multi-mode core. A fiber containing many (m) active single-mode cores allows two regimes of laser system operation:

1. Independent lasing in each of the m channels;

2. In-phase operation of all channels reached by any cophasing method.

For the same output power, the brightness (i.e., the far-field axial luminous intensity) of a fiber laser system with cophased channels will be m times higher than that of an arrangement with independently lasing channels. The phase locking techniques as applied to multi-core systems will be discussed below. We shall only note here that reaching a "perfect" cophased operation of a laser system for comparatively high output power and efficiency levels is practically impossible. In view of the sophistication and high cost of the cophasing techniques, engineers try to find a tradeoff between the requirements imposed on the performance of a fiber laser system and the possibilities of reaching in it a high radiation brightness.

A multi-mode fiber laser system can also operate in two “extreme” regimes:

1. Multi-mode oscillation

2. Fundamental mode amplification in the “master oscillator-power amplifier” arrangement using multi-mode fibers.

Obviously enough, in the first case one can easily attain the maximum output power, although with a large beam divergence (this situation is similar to the laser arrangement with many active single-mode cores but operated without cophasing). In the second case, the output beam divergence is very low, at the expense of reduced output power and energy efficiency of the laser system as a whole. Below we will discuss a number of issues associated with the multi-mode fiber-laser operation.

An analysis of the multi-mode fiber amplifier operated in the fundamental mode amplification regime at the maximum possible energy efficiency is very difficult to make. This operating regime depends on many factors. For instance, it is extremely sensitive to the optical quality of the fiber, to the pump launching efficiency, and to matching of the fundamental mode to the fiber profile. To illustrate this arrangement, we consider in the next Section a high-power laser system developed by Galvanauskas and Fermann.

High-Power Ultrafast Laser System Based on Fiber Amplifier

An analysis of the papers published in 2000 reveals that in some areas of quantum electronics double-clad fiber lasers begin to supplant the widespread and well-developed solid-state laser systems. In this Section, we are going to describe the results obtained by Galvanauskas and Fermann, which stand out among the other publications on the subject. During the recent decade, this research group has been intensively engaged in the problem of increasing the average and the peak power in fiber laser systems producing trains of ultrashort light pulses.

To increase the output power of a fiber laser system operating in a master oscillator-amplifier arrangement, Galvanauskas and Fermann proposed to use a multi-mode fiber core as a power amplifier, but with amplification of the fundamental mode only. The corresponding laser system was intended for generation of ultrashort (~100 fs) light pulses. The high peak intensities obtained in such systems with the wave propagating in a single-mode fiber give rise to strong nonlinear interaction. Starting from a certain wave intensity level, this interaction results in intolerable distortions of the light pulse and preclude its shortening. To reduce the intensity of the signal wave, it was proposed to use the fundamental mode of a multi-mode fiber with a large-diameter core (25 μm). For a given activator concentration in the quartz glass, this increase of the core diameter results in an increase of the limiting pump power P_{max} (19). Finally, if the G factor is kept constant, one will have to increase, simultaneously with the diameter of the core, that of the inner cladding as well, which, in its turn, facilitates the problem of launching the pump into the fiber.

Unfortunately, such laser systems cannot be constructed with long fibers, as is the case with single-mode fiber lasers. Excitation of higher-order modes in a fiber imposes an additional constraint on the length. Indeed, the fundamental mode can propagate in an ideal multi-mode core indefinitely without being scattered into higher-order modes. However, the imperfections present in the core give rise to mode coupling and can, hence, cause an intolerable degradation of the beam quality and of the ultrashort pulse shape. Propagation of the fundamental mode along the fiber may initiate the following mechanisms of higher-order mode generation:

volume Rayleigh scattering from random density fluctuations “frozen” into the quartz glass;

scattering and refraction on optical inhomogeneities at the interface between the core and the cladding;

birefringence in the fiber;

nonlinear refraction and nonlinear scattering;

amplifier excitation …..

As shown recently, using MOCVD technology to prepare fiber core rods with the desired configuration reduces substantially mode scattering in a fiber [61]. This technology was employed to develop fiber amplifiers with core diameters ranging from 25 to 50 μm, which allows stable single-mode oscillation along propagation lengths of up to a few meters. One of such fibers, 4.2 m long and with a core diameter of 25 μm (NA = 0.11, normalized frequency V = 16 for λ = 1055 nm), was used in the experiments of Galvanauskas and Fermann.

Figure 2 presents a fiber laser system generating ultrashort light pulses [62]. It consists of a fiber master oscillator generating a train of ultrashort light pulses, a single-mode compact fiber expander, an Yb-doped fiber power amplifier with a 25-μm core, and a pulse compressor. This laser system included a specially designed Er-doped fiber laser source [63], in which ultrashort pulses (a few fs long) with λ = 1550 nm were produced by the mode locking mechanism. Next, the radiation wavelength was Raman shifted in the fiber from λ = 1550 to 2100 nm, with subsequent frequency doubling (to λ = 1050 nm). In the Yb-doped fiber single-mode preamplifier, the average second-harmonic pulse power was raised to 300 mW, with simultaneous pulse chirping to 2 ps in length and ~20 nm in the frequency band.

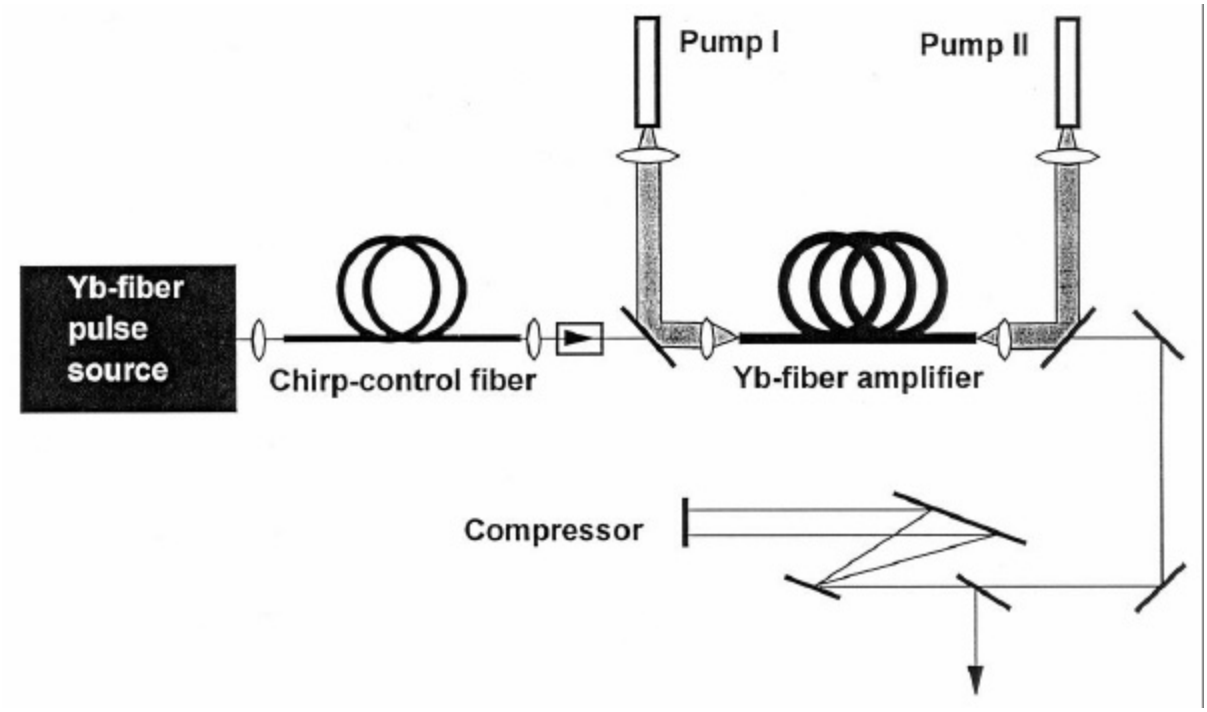

Fig. 2. Ultrafast laser arrangement based on a wide-band double-clad fiber amplifier pumped on both sides by laser diodes.

The fiber power amplifier, with the inner cladding 300 μm in diameter, is pumped from both ends by laser diodes operating at λ = 976 nm. The core/cladding area ratio was $G = 7 \cdot 10^{-3}$, which turned out to be large enough for efficient pump absorption over the short amplifier length. It was estimated that up to 14 W of pump power could be launched from either amplifier end, 97% of which were absorbed in the amplifier. Thus, the pump power per meter fiber length was about 6.5 W/m. This pumping level was obviously reached due to a more than sixfold increase of the multi-mode core in cross sectional area compared to the traditionally used single-core one.

Improvements in the techniques of this experiment raised the average laser output power to 5 W [62, 64]. A recent publication quoted a maximum average output power in this laser system of P_{out} = 13 W [65]. For a pulse repetition frequency f = 50 MHz, the output pulse energy reached 0.26 μJ. The efficiency of this fiber amplifier with a 25-μm core was estimated as 46%. The output beam was practically diffraction-limited (the measurements showed M^2 = 1.1). The beam peak power at the amplifier output was ~52 kW. It is pointed out that due to the positive dispersion of the fiber the length of the amplified light pulses increased as a result of the amplification from 2 to 5 ps, which permitted a more efficient pulse compression. At the output

of the laser system, the light pulses were compressed to 100 fs by a conventional compressor consisting of two diffraction gratings (600 lines/mm) spaced by ~10 cm. Thus, the peak power delivered by this laser system based on a fiber amplifier with a large-diameter core was 2.5 MW (with a high beam quality!). Note that this laser is considerably superior in performance to the commercial Ti:sapphire mode-locked oscillator, whose average output power is presently 2 W.

Galvanauskas and Fermann intend to further increase the average and the peak power output by choosing a fiber of a still larger diameter. They have already verified experimentally that a fiber amplifier with a core diameter of about 50 μm should provide stable single-mode operation. Increasing the core diameter and pump level should be paralleled by taking measures aimed at reducing the deleterious effects of the nonlinear processes which preclude reaching higher peak output powers. Galvanauskas and Fermann believe that this can be attained by chirping the light pulses launched into the power amplifier still more. It was pointed out [66] that the energy contained in the output light pulse (0.26 μJ) in the laser system considered is ~70% of the maximum energy limited by the onset of SRS at a given pulse length. Therefore in order to further increase the energy, one should stretch the light pulses launched into the power amplifier still more. The maximum light pulse energy is intended to be increased by increasing the length of the fiber used in the chirping. As follows from preliminary estimates, increasing the length of the fiber connecting the master oscillator with the power amplifier to 40 m should permit one to lengthen the pulses from 2 to 50 ps. Based on a numerical simulation of the oscillation in this laser system (Fig. 3), Galvanauskas and Fermann expect to substantially raise the average output power of their laser. Using a fiber core 50 μm in diameter, a more powerful pump system, and additional chirping, the average output power of the laser system can be expected to increase by a factor three to four, to reach 45--50 W [66]. It may be anticipated that compression of a more chirped pulse will increase the peak power at least by an order of magnitude to reach 25 MW. This value should apparently be considered as a limit for a fiber with such a diameter, because the specific instantaneous power density will in this case be $W = 1.27\ 10^{12}$ W/cm^2. At higher power densities the fiber material will suffer irreversible degradation. A study [67] dealing with the investigation of a new method of fabrication of connectors for a double-clad multi-mode fiber pointed out that at a power density $W_{max} = 1.5\ 10^{12}$ W/cm^2 (pulse length t = 100 fs, wavelength l = 790 nm) high-purity quartz undergoes plasma breakdown accompanied by a local change of the fiber refractive index. In doped quartz, the peak power limit is slightly lower.

Thus, the instantaneous power for the best samples of fiber lasers has already approached the level constrained by the limiting power density. The instantaneous power can be increased still more only by increasing the fiber cross section through the use of multi-mode or multi-core fiber. The average output power can be raised by a variety of means, including the one mentioned above.

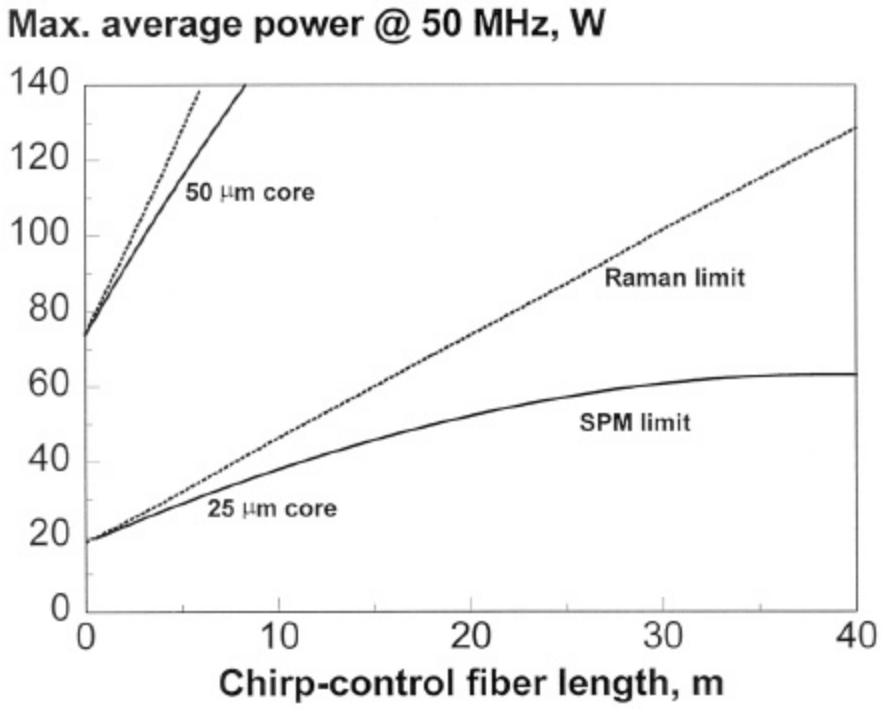

Fig. 3. Power scaling of a large-core fiber amplifier. Calculated maximum power for different chirp-control fiber lengths and two different fiber-core diameters. Solid lines – limitations imposed by selfphase modulation effects, dotted lines – limitation due to stimulated Raman scattering.

Scaleup of Double-Clad Fiber Lasers to High Powers Through the Use of Multi-Mode Fibers

When a single-mode fiber is used as a gain medium, the problem of the divergence of radiation does not naturally arise at all. The situation with multi-mode fibers is different. We encounter this case in trying to solve the problem of scaling up fiber lasers by increasing the core diameter. Note that single-mode lasing is actually not a very stringent requirement. For instance, some laser applications of a technological nature do not lay down such strict requirements.

The angular divergence of laser radiation is determined by the number and structure of the types of transverse oscillation modes. In optical fiber lasers, this structure is determined exclusively by the configuration of the fiber employed. The technique used to calculate the modes of weakly guiding dielectric fibers is well developed [68,69]. In a general case, finding the character of the intensity partition between the various modes which may participate in the lasing is a more complex problem. Because the solution of this problem requires the knowledge of the fiber mode structure, we are going to present here the main expressions from the theory describing the modes of a refractive-index step-profile fiber.

Let a be the radius of the cylindrical fiber core. Denote its refractive index by n1, and that of the cladding, by n_2. The propagation constant β for any fiber mode lies within the interval $n_1 k \geq b \geq n_2 k$, where $k = w/c$ is the wavenumber of free space. If we define the parameters as

$$u = \sqrt{k^2 n_1^{\,2} - \beta^2} \tag{21}$$

$$w = \sqrt{\beta^2 - k^2 n_2^{\,2}} \tag{22}$$

the mode field can be expressed through the Bessel function $J(ur)$ in the core, and by the modified Hankel function $K(wr)$ in the cladding. Besides the quantities u and w, one introduces one more parameter called the normalized frequency or the V factor:

$$V = a\frac{\omega}{c}\sqrt{n_1^2 - n_2^2} = ak\sqrt{n_1^2 - n_2^2} \tag{23}$$

The above parameters describing the guided mode in a fiber are related through

$$(au)^2 + (aw)^2 = V^2 \tag{24}$$

For $D = (n_1 - n_2)/n_2 << 1$, the case realized in practice, the field in the core can be presented as a superposition of linearly polarized modes, whose longitudinal components are negligible compared to the transverse ones:

$$E_x \propto [\sin(\nu\phi), -\cos(\nu\phi)] \begin{cases} J_\nu(ur)/J_\nu(ua) & r \leq a \\ K_\nu(wr)/K_\nu(wa) & r > a \end{cases} \tag{25}$$

$$E_y \propto [\cos(\nu\phi), \sin(\nu\phi)] \begin{cases} J_\nu(ur)/J_\nu(ua) & r \leq a \\ K_\nu(wr)/K_\nu(wa) & r > a \end{cases} \tag{26}$$

Because there is freedom of choice between $\sin(\nu\phi)$ and $\cos(\nu\phi)$, as well as two orthogonal polarization states, one may compile a set of four modes for each index ν. For $\nu = 0$, we have only two modes with orthogonal polarizations. The continuity conditions at the core-cladding boundary give rise to a characteristic equation, which, in its turn, brings about a multiplicity of discrete values of the propagation constant β and of the quantities u and w [69]:

$$\frac{J_\nu(ua)}{ua\,J_{\nu+1}(ua)} = \frac{K_\nu(\sqrt{V^2-(ua)^2})}{\sqrt{V^2-(ua)^2}\,K_{\nu+1}(\sqrt{V^2-(ua)^2})} \tag{27}$$

To simplify the calculations still more, we may use the fact that solutions with the same sets of indices, which relate to the x- and y-polarized components, are degenerate. For this reason, the superposition of these modes, whose intensity does not depend on the azimuthal angle, is also a mode of this system. It is the use of the latter modes that will permit us to restrict ourselves subsequently to the solution of a one-dimensional problem, with inclusion of the dependences of all the distributions on the radial direction only:

$$s(r) = C\begin{cases} J_\nu(ur)/J_\nu(ua) & r \le a \\ K_\nu(wr)/K_\nu(wa) & r > a \end{cases} \tag{28}$$

where C is a constant chosen from the normalization conditions.

After this short overview of the main results of the mode theory as applied to a dielectric fiber, we go over to a description of a multi-mode fiber laser model. In the case under consideration, the methods used to control the mode composition in bulk lasers are not applicable. This is why the paper [70] setting forth one of the most adequate models of quasistationary oscillation in a fiber laser is of a considerable interest. In this paper, an analysis was made of an end-pumped Nd:YAG fiber laser (a four-level system). The factors governing the mode composition of laser radiation in this model were the nonuniformity of the pump distribution over the fiber cross section and the spatial competition of various guided modes. The main attention was focused on the dependence of the threshold pump power for the given mode on the losses of this mode, and on the mutual position of the pump and mode distributions.

This model suggests the sequence of the steps that should be undertaken to reveal the conditions under which single-mode generation sets in in a multi-mode fiber. One looks first for the mode characterized by the lowest oscillation threshold for the given pump distribution. After this, one uses the above equations to calculate the threshold of two-mode operation of the arrangement. In this stage, the second mode is any mode of the set determined by the V factor. Obviously enough, if one maintains a pump level between the two threshold values obtained, the arrangement will operate in the single-mode regime.

We assume that the pumping is performed by a multi-mode source close in spatial characteristics to the Lambert source, or that the core is cladding-pumped. In this case, the pump distribution in the core is uniform. Hence, the normalized overlap coefficients introduced by the authors, whose magnitude depends on the mutual position of the pump and the mode, become the same for all the modes. In the model expounded in [70], it is these coefficients that determine the competition mechanism in the case of equal mode losses. Thus, for high enough pump levels, one cannot prevent the onset of multi-mode oscillation with simultaneous presence in the radiation of all potentially possible modes.

Note that this analysis has neglected the possibility of formation of a core in a double-clad fiber in which the doping ion distribution, rather than being uniform, will, for instance, vary smoothly in the radial direction. In this case, the spatial distribution of the pump rate will be determined not only by the pump mode composition, but by the spatial variation of the doping level as well.

Thus, if the pump is distributed uniformly over the fiber cross section, the laser intensity distribution over the transverse vibration modes will be uniquely determined by their spatial structure. Let us make an oversimplified calculation, which nevertheless will demonstrate the possibility of estimating the laser intensity distribution over transverse vibration modes in the case of uniform pump distribution over the core cross section. This calculation will simulate the cladding-pumped laser arrangement. In view of the foregoing, we shall assume the losses to be the same for all modes and to be due exclusively to the transparency of the output mirror. The characteristic numerical values of the physical quantities of interest to us here will be taken from [70].

The effective pump rate r(x,y,z) is, in a general case, a function of coordinates and accounts for the distribution of the inverse population density n(x,y,z). Taking wi(x,y,z) for the energy density distribution in the ith mode, the inverse-population distribution function n(x,y,z) takes on the following form, which can be readily derived from the rate equations for a four-level medium:

$$n(x,y,z) = \frac{r(x,y,z) \times t_2}{1 + \frac{cs\,t_2}{n_1 \cdot h\nu_s} \times \sum_{j=1}^{N} w_j(x,y,z)} \qquad (29)$$

We have used here the relation between the cross section of the process, the radiation intensity, and the transition probability per unit time $W = sI/hn$ (see, e.g., [71]). The last expression was derived assuming the relaxation time of the upper lasing level $\tau 2$ to be substantially longer than that of the lower lasing level $\tau 1$. Simultaneous presence in the system of N transverse modes accounts for the sum of N functions describing their spatial distributions. We have used here the following notation:

σ is the laser transition cross section;

$h\nu S$ is the energy of the photon emitted in the $2 \rightarrow 1$ transition.

The steady-state equation describing the balance of powers entering each mode in stimulated transitions and lost by radiation can be written

$$h\nu_s \int_{core} n(x,y,z) \frac{\sigma}{h\nu_s} \left[\frac{c}{n_1} w_i(x,y,z) \right] dv - \frac{?\delta}{2ln_1} \int_{cavity} w_i(x,y,z)\, dv = 0$$

where l is the length of the gain medium, and δ is the mode losses per resonator round transit. On substituting the inversed-population distribution function n(x,y,z) into the last equation, we come to

$$\frac{c\sigma t_2}{n_1}\int_{core}\frac{r(x,y,z)}{1+\frac{cs\,t_2}{n_1\cdot h\nu_s}\times\sum_{j=1}^{N}w_j(x,y,z)}w_i(x,y,z)\,dv=\frac{?\delta}{2ln_1}\int_{cavity}w_i(x,y,z)\,dv$$

Assuming uniform distribution over the core of the total power P_{abs} absorbed by the fiber as a whole, the last equation can be recast as

$$\frac{P_{abs}}{A}\frac{\sigma t_2}{h\nu_p}\int_{core}\frac{w_i(x,y,z)\,dv}{1+\frac{cs\,t_2}{n_1\cdot h\nu_s}\times\sum_{j=1}^{N}w_j(x,y,z)}=\frac{\delta}{2}\int_{cavity}w_i(x,y,z)\,dv$$

where A is the cross sectional area of the core.

The quantity $I_0 = hn_s/st_2$ is the saturation intensity, and the corresponding characteristic power density is $w_0 = n_1 I_0/c$. This quantity can be used to introduce the nondimensional power density of the ith mode:

$$u_i(x,y,z)=w_i(x,y,z)/w_0 \qquad (30)$$

We are turning now to the equations for the normalized power density distributions

$$\frac{P_{abs}}{A\cdot I_0}\frac{\nu_s}{\nu_p}\int_{core}\frac{u_i(x,y,z)}{\left[1+\sum_{j=1}^{N}u_j(x,y,z)\right]}\,dv=\frac{\delta}{2}\int_{cavity}u_i(x,y,z)\,dv \qquad (31)$$

We assume the transverse structure of the laser modes $s_i(x,y)$ to coincide with the distributions describing the fiber modes, in other words, we shall neglect mode distortion. While appearing reasonable, this assumption certainly requires validation.

$$u_i(x,y,z)\approx s_i(x,y)\cdot g_i(z)$$

Moreover, as done in [70], we shall consider, for the sake of simplification, the case of approximately uniform mode intensity distribution along the fiber. Then

$$\int_{cavity}u_i(\vec{r})dv=\int_x\int_y s_i(x,y)dA\cdot\int_l g_i(z)dz=g_i\cdot l\int_x\int_y s_i(x,y)dA=\frac{1}{w_0}\int_{cavity}w_i(\vec{r})dv$$

and normalizing the transverse distribution of any mode $s_i(x,y)$ in such a way that

$$\frac{1}{A}\int_x\int_y s_i(x,y)dA=1 \qquad (32)$$

we obtain

$$g_i=\frac{1}{Alw_0}\int_{cavity}w_i(\vec{r})dv \qquad (33)$$

The last expression suggests that the quantity gi is the normalized energy of the ith mode. The ratio of the lasing to pump frequency is the so-called pump quantum efficiency. In real lasers, the pump efficiency ηp is less than the quantum efficiency, and therefore in the final expression we shall use this quantity and the pump power Pp:

$$\frac{1}{A}\int_A \frac{s_i(x,y)}{\left[1+\sum_{j=1}^{N} s_j(x,y)\cdot g_j\right]}\,dA = \frac{\delta}{2P_p}\frac{1}{\eta_p}A\cdot I_0 \qquad (34)$$

The numerical values of the physical quantities used are n1 = 1.820, n2 = 1.815, λS = 1.064 μm,
σ = 3.2×10-19 cm2, τ = 230 μs. To have a grasp of the order of magnitude of the quantities we are going to deal with, estimate the characteristic power $A\cdot I_0$, through which one can readily express all the other characteristic quantities. For instance, for a core radius a = 2.0 μm we obtain for the characteristic power $A\cdot I_0 \approx 3.2\times10\text{-}4$ W.

We start with the case of single-mode oscillation. For the core radius we choose a = 2.0 μm. This yields V ≈ 1.59223 and, hence, for the given frequency the fiber is single-mode, because V < 2.405 [69]. For ν = 0, the characteristic equation (27) yields a mode whose normalized power density distribution is plotted in Fig. 4. The modes are conventionally labeled using two indices, the first of them being the azimuthal number ν, and the second, a positive integer discriminating different solutions for a fixed ν. For the sake of simplicity, we shall label the modes in the order in which they appaer in our consideration. Thus, the mode treated here acquires index 1.

Recalling Eq. (34), the equation for the single-mode regime takes on the form

$$\frac{1}{A}\int_A \frac{s_1(x,y)}{\left[1+g_1\cdot s_1(x,y)\right]}\,dA = \frac{1}{P_p}\frac{\delta\cdot A\cdot I_0}{2\eta_p} \qquad (35)$$

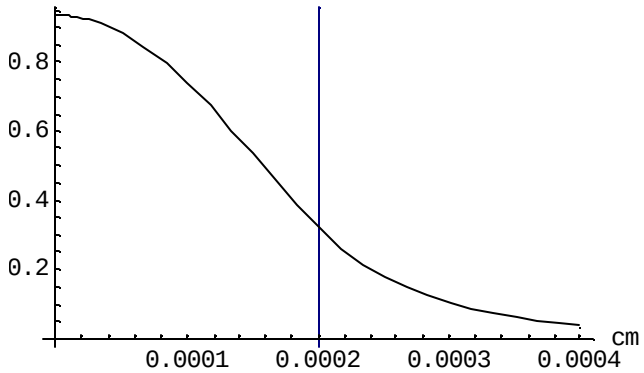

Fig. 4

Obviously enough, the expression for the threshold pump power can be obtained from (35) by substituting $g_0 = 0$. Then for the threshold pump power in the mode under consideration we obtain

$$\left(P_p\right)_{th,1} = \frac{1}{\gamma_1}\frac{\delta A I_0}{2\eta_p} \equiv \frac{1}{\gamma_1} P_{th}$$

where

$$P_{th} = \frac{\delta A I_0}{2\eta_p}$$

and the integral

$$\gamma_1 = \frac{1}{A}\int_A s_1(x,y)dA \qquad (36)$$

characterizes the degree to which the core cross section is filled by the mode. For instance, in our case $\gamma 1 = 0.5878$. Note that the mode oscillation threshold depends on the core filling γ by the mode. Indeed, the smaller is this filling, the higher has to be this threshold. Finally, if one uses a normalized coordinate $\rho = r/a$, and the power is measured in units of Pth

$$p = P_p / P_{th} \qquad (37)$$

equation (35) takes on the form

$$2\int_{\rho=0}^{1} \frac{s_1(\rho)\cdot\rho\cdot d\rho}{\left[1+g_1\cdot s_1(\rho)\right]} = \frac{1}{p} \qquad (38)$$

The left-hand part of this equation, which can be readily calculated, is a function of parameter g_1, whose value is determined by the pumping. Figure 5 displays graphically this $g_1(p)$ relation.

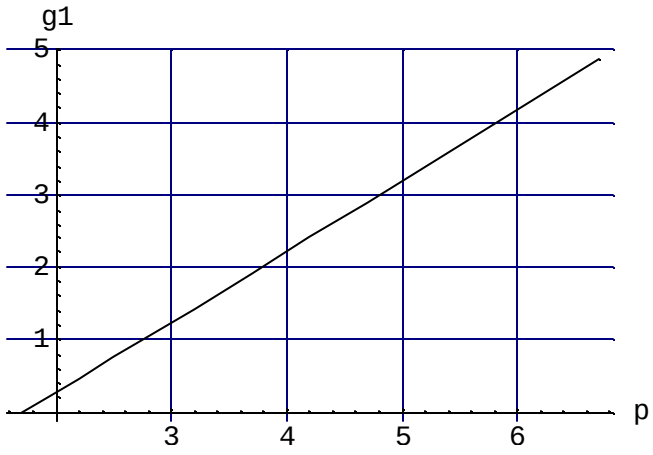

Fig. 5

Let us turn now to multi-mode oscillation. The coupled equations for N simultaneously oscillating modes can be written

$$2\int_0^1 s_i(\rho)\left[1+\sum_{j=1}^{N} s_j(\rho)\cdot g_j\right]^{-1}\rho\, d\rho=\frac{1}{p} \qquad i=1,2,....N \qquad (39)$$

Consider the case where the fiber can support two guided modes. This situation is realized, in particular, in a core of radius a = 4.0 μm. The normalized frequency is V ≈ 3.18446, which confirms the multi-mode nature of the core at the given oscillation frequency. Indeed, the solutions of the characteristic equation (27) yield two modes. For ν = 0, one obtains a mode with the maximum at the axis. For this mode, γ1 = 0.91105. The second mode, with the index ν = 1, has a minimum at the axis, and γ2 = 0.711748. The normalized radial power density distribution of these modes is plotted in Fig. 6.

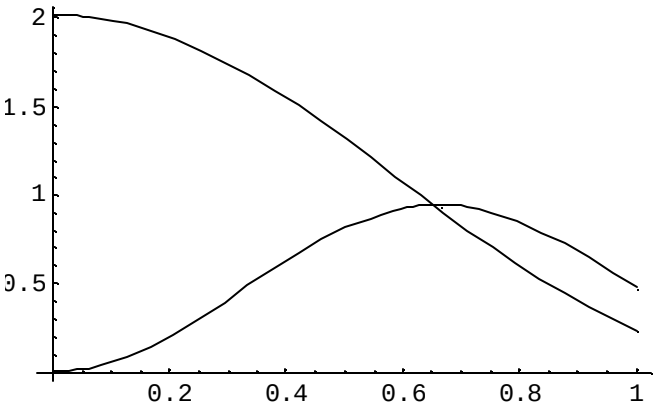

Fig. 6

When solving Eqs. (39), one has to bear in mind that the quantities g_1 and g_2 of interest to us here, which are normalized mode energies, must obviously be positive. Thus, physically meaningful solutions obtained when using the two equations lie in the pump range where g_1 and g_2 are positive. Obviously enough, this will occur after the second mode forms in the oscillation. The pump power range from the threshold of the first mode to that of the second is described by the solution of Eq. (38) for the single-mode case. The results of the relevant calculation are presented graphically in Fig. 7.

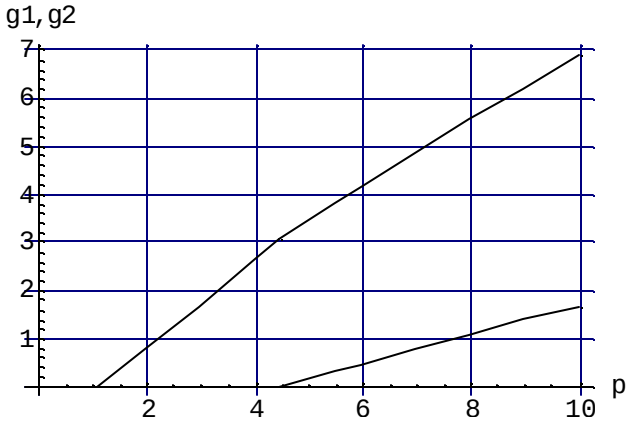

Fig. 7

The weakly pronounced break in the pump dependence of the first-mode energy is due to the first mode suppressing efficiently the formation of the second mode. Indeed, if the first mode had been absent for some reasons, the second-mode threshold would be 1.405, which is about

one third of the calculated threshold. In actual fact, at the instant of formation of the second mode the first one, which is already fairly strong, suppresses its development.

The calculations have demonstrated that in some cases the multi-mode fiber laser operation can be efficiently suppressed by spatial mode competition in the multi-mode fiber. We stress once more that the power distributions of the modes considered here overlapped fairly weakly. As already mentioned, the maximum of the first mode lies at the minimum of the second, and the maximum of the second mode is located at the weak tail of the first one. One may naturally ask how would the energy distribution pattern of the two modes change in the case of a stronger overlap. It appears of interest to consider the situation of the presence of two modes with an azimuthal index $\nu = 0$.

We increase the core radius still more, to a = 6.0 μm. We obtain $V \approx 4.7767$. The curves corresponding to the right- and left-hand parts of the characteristic equation (27) are presented in Fig. 8 for $\nu = 0$.

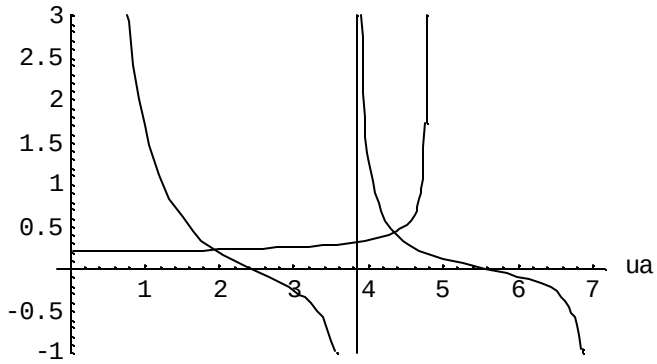

Fig. 8

An increase of the core radius gave rise to two curve crossings. Each of the crossing points determines a guided fiber mode. Figure 9 illustrates the normalized power density distribution for these modes. In addition to the two distributions shown in Fig. 6 (modes 1 and 2), we have now one more, with the maximum at the core axis (mode 3).

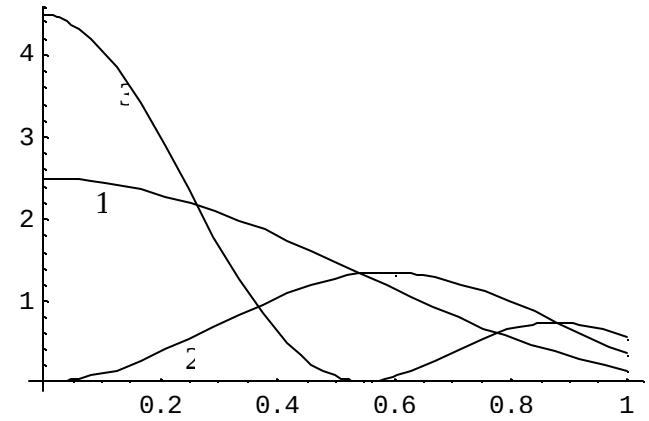

Fig. 9

The calculation was carried out by the technique used in the two-mode case. First of all, we find the pumping at which all three modes appear. In our case, at the pumping level p = 212.7

the mode energies are g1 = 50.22, g2 = 161.177, and g3 = 0.0007. Starting from this value, only the first and second modes will oscillate at lower pumping levels. The subsequent calculations will follow the same procedure. Figure 10 displays the normalized energies of modes 1 and 2 versus pumping level, calculated in the pumping range where the third mode formed. The energy of mode 2 in this range is always higher than that of mode 1. Because the energy of mode 3 turned out to be two orders of magnitude lower than that of modes 1 and 2, the corresponding energy dependence is presented in a separate plot (Fig. 11).

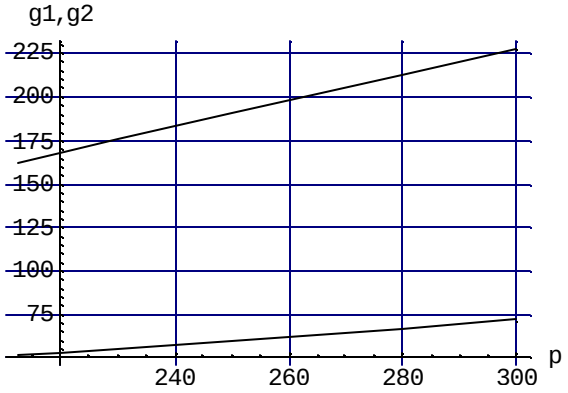

Fig. 7 $g_2 > g_1$

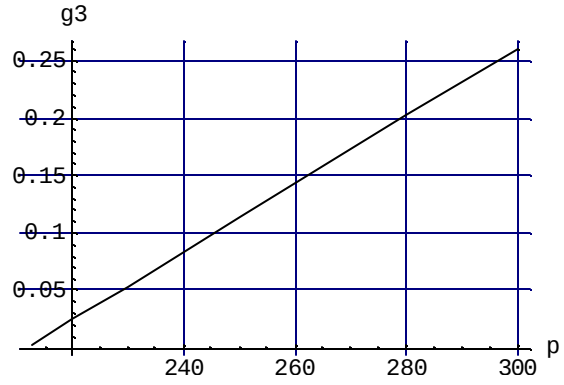

Fig. 8 g_3

Thus, for the fiber parameters chosen, spatial mode competition results in such a strong suppression of mode 3 that we have here actually two-mode laser operation. The reason for this behavior of the system is fairly simple; as seen from Fig. 9, mode 3 occupies primarily the core central zone and fills very inefficiently the core volume. This is indicated by the mode filling coefficients of the core: $\gamma 1 = 0.9678$, $\gamma 2 = 0.9087$, $\gamma 3 = 0.7132$. As a result of the filling coefficients of the first two modes being similar, their thresholds nearly coincide. Figure 12 displays the pump dependences of their energies for the system operating in the two-mode regime, and Fig. 13, the same dependences near the threshold.

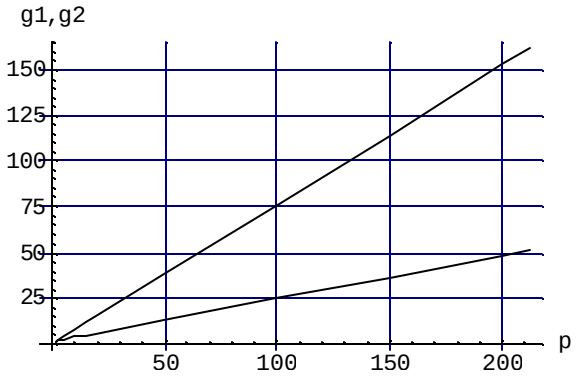

Fig. 12

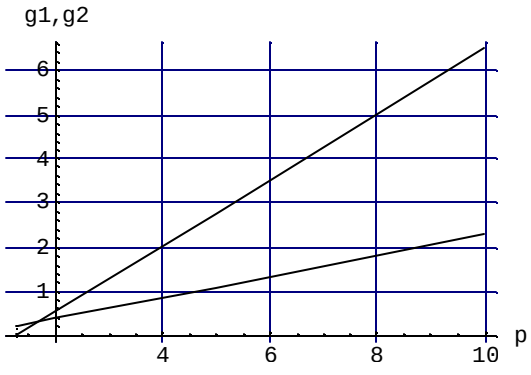

Fig. 13

Using Multi-Core Fibers

An attractive alternative to multi-mode fibers in an attempt to increase the output power is to use instead several single-mode cores combined in a common cladding, through which the pump radiation is guided. The single-mode composition in each channel is ensured by properly choosing the corresponding doped-fiber parameters. The beams produced in different channels are summed at the output, in a phase-locked or random manner. Progress achieved in the technology of manufacture of such fibers provides favorable conditions for research in this direction. There are several publications on multi-core fiber lasers. In this part of the Report, we are going to consider briefly the problems encountered in the development of lasers of this kind.

As stated above there exists the maximum possible specific pumping of the doped core, which is determined by the fluorescence decay time and the dopant concentration. As already mentioned, this problem can obviously be solved by increasing the doped core volume. Therefore to increase the laser output power, one uses in some cases multi-mode fiber, the subject treated in the preceding Section.

Another way to increase the gain medium volume of a fiber laser lies in using a bunch of single-mode fibers encased in a common cladding. In this configuration, the single-mode doped fibers are distributed in a certain manner in the cladding. The optimum geometry of their arrangement can be determined by computer simulation of the processes occurring in oscillation. Among the obvious merits of this geometry is the simplicity of

- reaching uniform illumination of the cores by the pump radiation;
- achieving uniform heat removal;
- providing compact launch and coupling out of the radiation from the fiber.

The same conclusion was reached in [72], where one proposed a geometry, in which doped single-mode cores are arranged in the periphery of the cladding. This arrangement is called M-configuration fiber. Figure 14 shows the cross section of, and the refractive index distribution in an M-configuration, double-clad fiber having 24 single-mode cores.

An analysis of the pump field configuration [72] provided supportive evidence for the peripheral fiber zone being the best location for periodically arranged single-mode cores. In this case, the mi;ti-mode pump radiation feeds uniformly the doped cores. In this geometry, there are practically no trajectories along which pump rays could pass past the single-mode cores, which is possible in an axially symmetric cladding with a central core.

One more merit of this geometry is that the main heat sources (the doped cores) lie in the periphery of the fiber, with the heat being removed from the outer fiber surface. Thus, in this geometry the temperature is maximum in the central part of the fiber, where the pump propagates. By contrast, in the region of the doped cores the temperature is the lowest, and the temperature gradient, the largest. The "overheated" central part practically does not affect propagation of the pump along the fiber. At the same time the lower temperature of the doped cores, when compared to the central core arrangement, results, in its turn, in a weaker quenching of the heating-induced fluorescence. The fact that the temperature gradient is maximum in the peripheral zone will not apparently produce anything but a slight effect, and, given the small diameter of the doped cores, their deformation should be small and not affect noticeably the quality of the generated radiation.

Until very recently, the main obstacle to experimental investigation of such fibers with a large enough length has been the difficulty of their fabrication. One has succeeded [72] in fabricating only two experimental samples (Figs. 14b,c), but only in one of them (Fig. 14b) the 40 single-mode cores, 5 μm in diameter, were doped with Nd^{3+}.

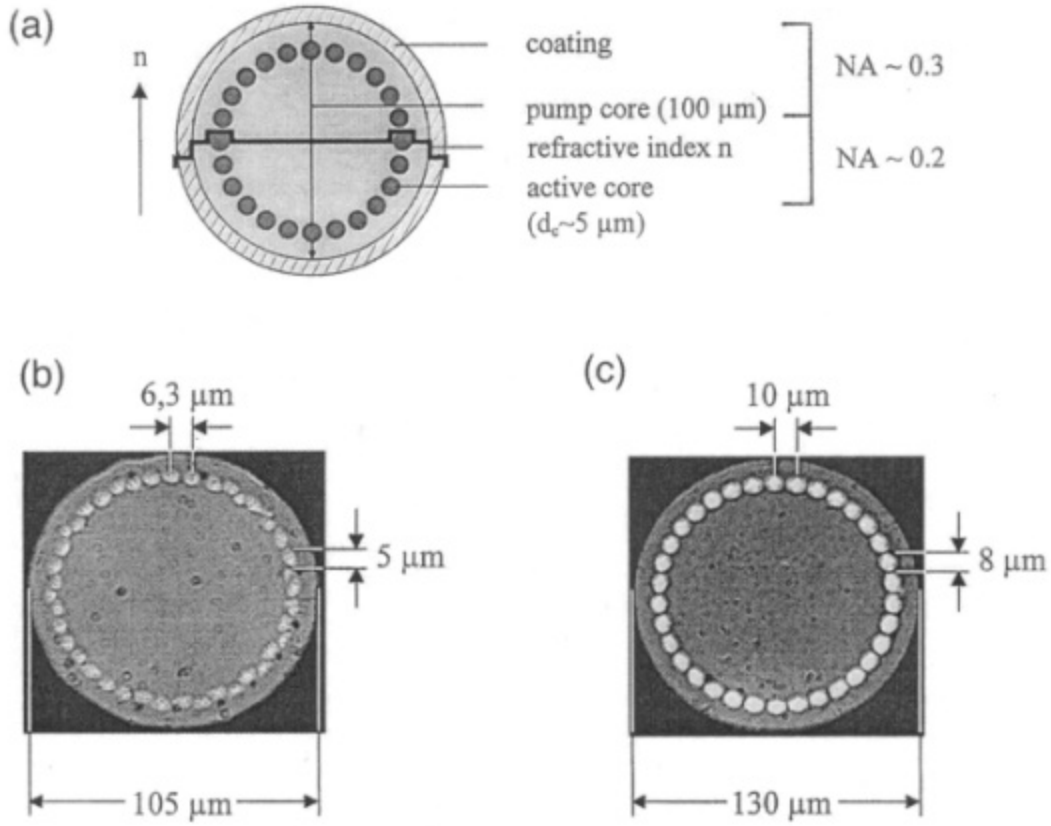

Fig. 14 (a) Layout of a multicore M-profile fiber including the refractive index distribution. (b) Realised multicore fiber with 40 Nd –doped single mode cores. (c) Realised multicore fiber with undoped cores.

Note that the total cross sectional area of the Nd^{3+}-doped fiber arranged in the M configuration was S_{eq} = 0.0008 mm². This area is half as much again the area of the fiber used by Galvanauskas and Fermann (S = 0.0005 mm², d = 25 μm) in their experiments on amplification of the lowest mode in a multi-mode fiber [73]. Besides, in their experiments the length of the multi-mode fiber could not exceed the limit above which higher-order modes would be excited. M-profiled fibers are free of this constraint on the fiber length. Thus far, the constraints met here originate only from the technological problems encountered in the fabrication of such fibers. However, there is a possibility of making composite fibers.

The output power of such a multi-core fiber laser is obviously proportional to the number of the single-mode cores arranged in one cladding. As the number of the single-mode cores increases, the diameter of the cladding in which the pump is guided increases too. This permits one, in its turn, to increase the pump power launched into the cladding proportional to the core number. A significant merit of an M-profiled fiber is that for a large number of single-mode cores and, accordingly, a large cladding diameter one can use low-brightness diode arrays for pumping the laser system.

The only serious shortcoming of the geometry considered is apparently the incoherent summation of the beams produced by individual single-mode cores at the laser output.

Overcoming this disadvantage will require taking special measures aimed at beams phase locking.

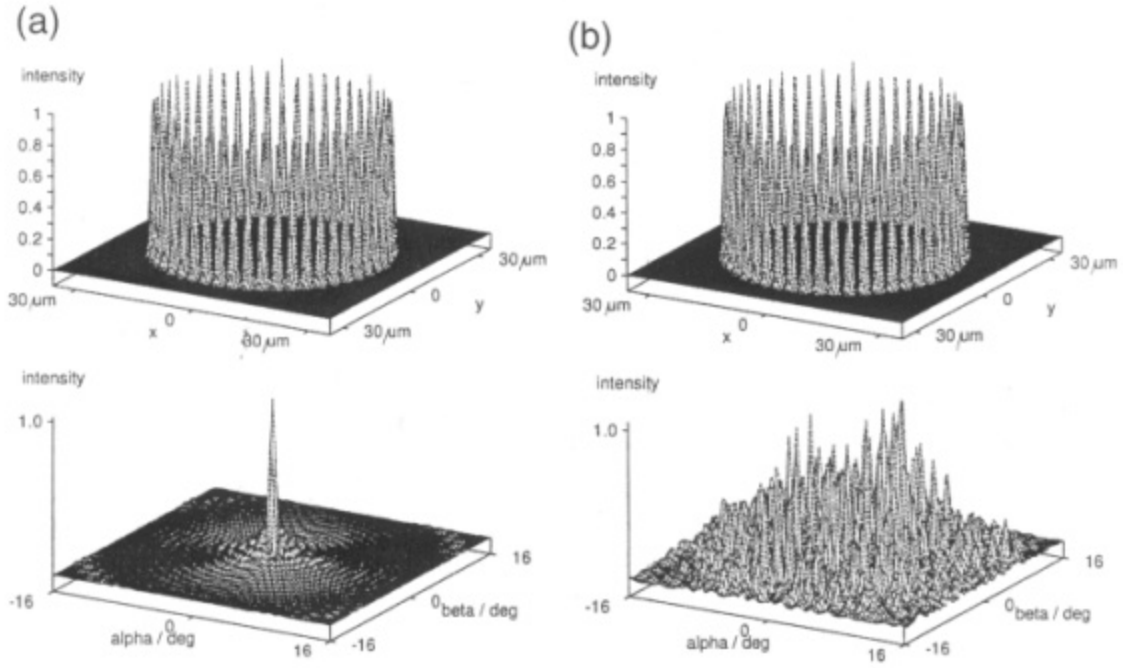

Fig. 15 (a) Normalised near- and far-field distributions for an array with in-phase coupling. (b) Normalised near- and far-field distributions for an incoherent array.

Figure 15 shows near- and far-field distribution patterns for two cases, namely, for single-mode emitters operating in the phase-locked (Fig. 15a) and dephased (Fig. 15b) regimes. Note that the far-field distribution is displayed in arbitrary units. To compare the far-field distributions, one should take into account that in the case of coherent summation of the output beams produced in separate channels the axial radiation intensity scales as the square of the number of channels. In our opinion, a high brightness of such a multi-channel laser can be provided in two ways.

In the first version, two conditions should be met: one should achieve the same optical length in all single-mode channels and provide mode locking by making possible penetration of the radiation between the neighboring cores.

In the sceond version, conversely, one should prevent radiation from penetrating from one channel to another, after which one could use the phase conjugation (PC) method to match the beams exiting individual channels in phase using the well-known arrangement of the double-pass amplifier with a PC mirror. We shall consider the possibility of using the PC technique to increase the brightness of fiber lasers in the final Report. We shall now discuss briefly the technique involving coupled modes generated in closely spaced single-mode channels.

The energy exchange between neighboring waveguides was described well enough using coupled-mode equations [74] in the weak coupling approximation. However, as established in [75,76], to reach phase locking in an M-profiled fiber, the modes excited in neighboring cores should be coupled as strong as possible. Besides, the refractive index distribution is in practice usually more complex than the one assumed in analytic theory. These two considerations make one turn to numerical calculations. A comprehensive numerical investigation of propagation in a cylindrical multi-core fiber of M-configuration was carried out in [76]. The calculation of parameters of a concrete fiber laser should undoubtedly be done by the technique developed in

[76]. For a qualitative description of mode coupling betwen adjacent channels we shall use here the results of an approximate analytic treatment [72,77].

In the case of a close-packed core array, where the distance d between the centers of the cores is comparable to their diameter a, a Gaussiam beam of width w (at the $1/e^2$ level) propagating along a core penetrates into other channels. Such injected beams give rise to cross coupling in laser channels. A number of papers discuss the magnitude of the coupling k between neighboring channels [72,74-77].

Figure 16 plots the behavior of the k coefficient presented in [72]. The positive values of k relate to the case where the beams in adjacent channels are in phase, and the negative ones, when they are in opposite phase. Note that under certain conditions $k = 0$. In this case, oscillation in different channels occurs independently, and for such fiber parameters the brightness can be increased by phase conjugation.

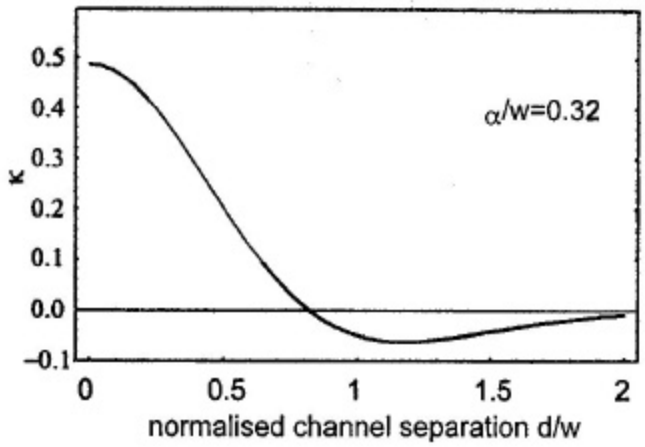

Fig. 16 Coupling coefficient k depending on the normalised channel separation d. (d is in units of w, the $1/e^2$ width of the laser field intensity).

The above expression for the coupling coefficient k is valid as long as the channels are equivalent, pumped to the same extent, and the longitudinal modes do not spread out. When these conditions are not met, one cannot obtain a high-quality output beam with a quasiplane wavefront. In this case one can only match in phase the beams exiting neighboring channels, but only in the sense that phase fluctuations in one channel initiate the corresponding fluctuations in other channels.

Thus, to reach phase-locked operation in a multi-core fiber system, several conditions have to be satisfied. First, one has to arrange cores in a certain geometry and provide the same pumping conditions in all the channels. Nonlinear processes, which may destroy mode locking, have to be suppressed. These conditions can apparently be met. Second, the single-mode cores have to be optically equivalent. Indeed, it is difficult to avoid in the course of the core manufacture refractive index variations along the fiber and, as a consequence, different optical lengths of the oscillation channels. If the operational parameters of an M-profiled fiber laser (the pump level, heat removal regime, static fiber position etc.) are fixed, it apparently is possible to use a static corrector to level the optical lengths of all single-mode cores. No such studies have been reported in the literature, and this proposal should be considered only as a possible solution to the above problem.

Finally, let us turn to the experimental results obtained on M-profiled fibers. The experiments discussed in [72] were done on a fiber containing 40 Nd^{3+}-doped single-mode cores arranged in

the periphery of the cladding (Fig. 14b). The present technology level has permitted one to fabricate only a 40-cm section of such a fiber. The maximum average output power of such a laser was 0.45 W. Unfortunately, because of imperfect technology, the passive losses in cores were 25 times higher than those in standard Nd^{3+}-doped fibers. The average specific output power of 11 W/m can be increased in the future by reducing the losses and optimizating the parameters of the resonator and of the pump launching system.

As seen from Fig. 16, in the multi-core fiber studied in [72] ($d/w \sim 0.39$ and $a/w = 0.32$), the modes excited in adjacent channels could be strongly phase coupled. However, the divergence of the output beams of the 40 channels did not differ from that of one channel, which implies incoherent summation of the channels in these experiments. The studies of the near-field pattern revealed the reason of the poor quality of the net beam; it was found that the conditions of oscillation in various channels were noticeably different.

Despite the unsatisfactory results of the first experiments on coherent summation of beams from single-mode cores enclosed in a common cladding, it is in this direction, which has just started developing, that one may hope future progress to occur.

On Increasing the Beam Brightness by Means of Linear and Nonlinear Adaptive Optics

For several decades already, linear adaptive optics and phase conjugation (PC) methods have been attracting intense interest of specialists in their potential for increasing the brightness of output radiation in laser systems. The question of the extent to which the use of these methods of wavefront correction in lasers is expedient remains open. The fact is that such laser systems grow extremely complex and unreliable, and their efficiency decreases substantially.

Optical distortion compensation in fiber lasers with a PC mirror

Information on the use of the PC techniques in fiber lasers is so scarce that in our analysis we had to invoke the experience gained in applying PC to lasers of other types. Therefore we would like first to present two examples of the use of PC techniques in lasers operating in the 10- and 1-μm ranges.

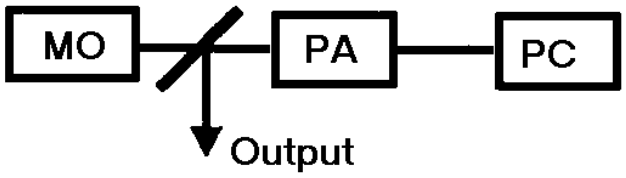

Fig. 17. Block diagram of experiment to study a double-pass amplifier with a PC mirror (MO - master oscillator, PA - power amplifier, PC - PC-based mirror).

Successful use of nonlinear optics can be exemplified by an experimental study of a double-pass amplifier with a PC mirror (Fig. 17) performed on a high-power repetitively pulsed CO_2 laser [78]. These experiments were crowned by achieving parameters which are apparently record high for lasers of this type. The pulse energy reached 1 kJ at a pulse repetition frequency of 50 Hz, and the beam divergence was only twice the diffraction-limited value. However, despite the high average output power and a good beam quality, the laser reliability was poor, because the optical arrangement was made up of about 100 components. Besides, the laser efficiency decreased by nearly an order of magnitude compared to the same laser having a standard resonator with optimum feedback. In other words, the question of whether the use of PC in a high-power repetitively pulsed CO_2 laser is practical still does not have a clear-cut answer.

The situation with the application of PC to industrial lasers in the 1-μm range is in no way better than in the 10-μm one. Comprehensive relevant studies were carried out by a group of scientists headed by Eichler at Berlin University. Year after year, the output power of the solid-state PC system, which Eichler with colleagues was building with a view for industrial applications, was increasing. One succeeded in reaching a high average output (Pout = 104 W) of the laser system with a PC mirror and a practically diffraction-limited beam divergence (M^2 =1.2) [79]. The latest reports submitted by Eichler at a number of conferences quoted output power figures for his laser as high as W = 500 W and more. This time, however, the output power amplifiers were not included in the PC compensation loop because of the difficulties involved in its use. This "simplification" of the circuit was a forced step, despite the well-known fact that it is in these elements that most of the optical distortions arise.

Thus, the above examples show that application of nonlinear optics to wavefront correction in laser systems is still a subject of controversy. As for the fiber lasers, the direction which has been rapidly developing in recent years, nonlinear optical compensation of their output wavefront has been studied only in a small number of papers (see, e.g., [80,81]). By contrast, using the fiber itself as a medium for an SBS PC mirror has been discussed by many authors {e.g., [82]); this subject is, however, beyond the scope of our consideration.

Experience gained in operating lasers of other types suggests that the double-pass power amplifier with a PC mirror (Fig. 17) is practically the only arrangement applicable to fiber lasers. The PC mirror arrangement (Fig. 18) turned out to be difficult to adjust and does not enjoy application in lasers other than those with a loop resonator [83]. True, three years ago Eichler announced that he was planning an experimental study of a laser with a PC mirror and a gain medium based on a multi-mode fiber [79]. By his estimates, the output power of such a laser should exceed 50 W. No information on the results of this study, however, has been published thus far.

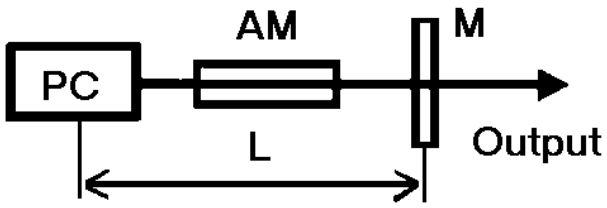

Fig. 18. Block diagram of a resonator with a PC mirror (M - output mirror, GM - gain medium, PC - PC-based mirror).

PC techniques can be applied to advantage only to reciprocal optical systems. In the case where the beam passes in both directions, distortions build up in the wavefront, and the idea itself of a double-pass amplifier with a PC mirror looses any sense. An optical system can become nonreciprocal as a result of such irreversible and nonlinear processes as

- diffraction,
- stimulated scattering,
- mode coupling,
- gain saturation, etc.

A single-mode fiber may be considered, in a certain approximation, as a reciprocal optical system. If there is no stimulated scattering and fiber coupling (see above), a bundle of single-mode fibers may also be regarded as a reciprocal optical system. Thus, it can be maintained that using, for instance, an M-profiled fiber in a laser with a PC mirror appears to be more promising than application of a multi-mode fiber in the same arrangement. The fact is that mode coupling plays a major role in a multi-mode fiber. Even the slightest vibration of such a fiber exerts a strong effect on the field redistribution dynamics among the various modes. Besides, the light field distribution in a multi-mode fiber is very sensitive to the way in which the beam is coupled into the fiber. For instance, the optical path difference between single-mode channels in an M-profiled fiber can vary slowly in time under certain conditions. The optical path difference between individual single-mode channels in such a fiber has two components, more specifically, a static one determined by imperfect manufacture, and a dynamic one, originating from the fibers being at different temperatures during the laser operation. Obviously enough, for fixed pump and heat removal parameters one can attain in an M-profiled fiber a practically static pattern of wavefront distortions of the beam passing along it. This is an essential point, because

the wavefront distortions to be compensated have to be "frozen" for the time interval needed for the PC mirror to respond.

One can find in literature theoretical and experimental studies of wavefront correction in fiber lasers by means of a PC mirror.

A theoretical analysis of phase matching of the beams produced by individual single-mode fibers can be found in [80]. It is pointed out that, despite a complex character of the signal wave, the reflectivity of a quarter-wave mirror employed may reach a high value. About 50% of the pump radiation coupled into a PC mirror can be launched into a fiber to be amplified in the back transit. One determined also some conditions necessary for phase matching of individual channels. The paper does not, however, discuss the possible decrease of the reflectivity and compensation fidelity caused by the inertia in the hologram recording in a photorefractive crystal.

Ref. [81] discusses in considerable detail a double phase-conjugate mirror (i.e., a mirror for phase conjugation of two signal beams) making use of a photorefractive medium. This mirror does not need an additional pump. The hologram employed to diffract the two signal waves into conjugate waves is recorded by the signal waves and a seed wave of the background noise origin. Obviously enough, such a mirror can be realized in a highly sensitive crystal in which large variations of the refractive index can be attained. Figure 3 illustrates the results of an experiment demonstrating the applicability of such a mirror to a fiber laser. However, no information on the energy and temporal characteristics of the PC mirror are quoted in [81]. The PC mirrors in the above studies are operated in the pulsed or repetitively pulsed modes. At the same time, fiber lasers are frequently employed in CW or quasi-CW operation.

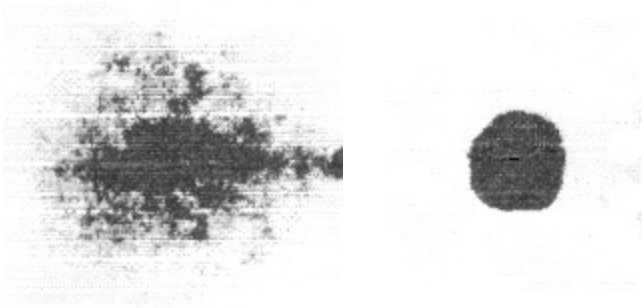

a **b**

Fig. 19. Operation of a double phase-conjugate mirror: far-field intensity distributions of (a) signal-wave and (b) output beam after the PC compensation.

We believe that progress in wavefront correction in a multi-fiber quasi-CW system can be reached using the Zernike cell [84]. Such a PC mirror has a number of merits:

1. a high reflectivity (ultimately 100%);
2. inertialess response;
3. preferable when operating with CW or quasi-CW radiation;
4. the mirror operates irrespective of the actual state of signal-wave polarization;
5. the mirror provides phase conjugation of monochromatic radiation of any wavelength, but known in advance.

For such a mirror to operate properly, two conditions should be met:

- wavefront distortions should not be large and of a scale size small compared to the beam aperture;
- the signal-wave far-field intensity distribution should have a distinct core (maximum peak), whose radiation is directed along the axis of the Zernike cell.

These conditions can be satisfied in an M-profiled multi-fiber laser system. The optical path difference between the various channels, due to imperfect manufacture or arising in the pumping of single-mode fibers, can be compensated using a static corrector tailored specifically for this purpose. Small dynamic and residual static wavefront perturbations will automatically reverse their sign on reflection from the Zernike cell. Note that the laser arrangement should have a fast enough adjusting device to direct the core of the beam onto the center of the Zernike cell reflector. Present-day technology will offer easy solutions to this problem.

Note that we have not met in the literature descriptions of such a fiber laser with a Zernike cell-based PC mirror. In our opinion, this arrangement deserves further theoretical and experimental study.

Using Linear Adaptive Optics in Fiber Lasers

Correction of dynamic phase distortions by linear adaptive optical systems reduces to the use of a properly controllable mirror provided by a large enough number of discretely arranged pistons (actuators). Such systems have been attracting considerable interest for a long period of time and are presently applied with success in a variety of optical instruments. At the same time, these systems possess certain properties that place a constraint on their application. Among them are:

1. a fairly large mass and size;
2. a large number of drives, a factor reducing the reliability of a system as a whole;
3. a limited dynamic range;
4. a limited scale of distortions that can be compensated;
5. complexity of information transfer and mirror control in real time, even using a fast computer.

In the cases where only a few tens of channels have to be compensated, this arrangement may be considered feasible. It is this situation that is met, for instance, in a fiber laser with the M-profiled gain medium mentioned earlier. This system can use for a mirror (or phase modulator) spatial light modulators (SLMs), segmented piezo-mirrors, or miniature microelectromechanical correctors (MEMS), which are presently intensively developed [85]. The control signals for the corrector can be produced by heterodyning, a technique employed currently with considerable success [86]. This technique permits one to measure, very fast and with a high precision, the phase deviation in each channel relative to a laser source operating at a highly stable frequency. We have not thus far located in the literature any information on experimental investigation of such a multi-channel fiber laser with linear adaptive correction. Such studies will hopefully be carried out at TRW, whose researchers have recently submitted in Europe a patent with the following formula [87]:

A high average power fiber-laser system comprises a master oscillator for generating a primary laser signal; a beam splitter array for splitting the primary laser signal into N secondary laser signals; an optical frequency shifter for shifting the frequency of the primary laser signal; a phase modulator array for providing phase compensation of the N secondary laser signals; N single-mode dual clad fiber amplifiers for amplifying the N secondary laser signals and generating an output beam; a beam sampler for sampling the wavefront of the output beam, defining an array of sampled signals; means responsive to the array of sampled signals for interferometrically combining the array of said sampled signals and the shifted primary laser signal into an array of heterodyne optical signals, each having a phase that corresponds to the state of phase of the array of sampled signals; and means responsive to the array of heterodyne optical signals for providing a plurality of feedback signals to the phase modulator array that are linearly proportioned to the state of phase over at least one wave to provide phase compensation of the secondary laser signals. This includes digital dividers for dividing electrical signals by a selected integer and an exclusive OR gate for providing a pulse train having a duty cycle that reflects the phase to be compensated.

To sum up, it may be concluded that work on the application of PC mirrors and linear adaptive optics devices to fiber lasers is still in its infancy, and it would be premature to make presently any forcasts on the feasibility of their future use.

Conclusions

The work carried out can be summed up as follows:

1. In the current state of fiber laser development, thermal effects do not constrain their output power;

2. Saturation of the activator concentration in the fiber core and the fairly low brightness of laser diode arrays impose a constraint on the specific fiber pump power;

3. When operating in the ultrashort pulse regime at high peak power levels in the gain medium, the laser power can be constrained by the SRS and selfphase modulation effects in the fiber.

4. In our opinion, the problem of high-power scaling of fiber lasers can be most efficiently solved by using various large-core fiber arrangements (multi-core single-mode fibers and multi-mode fibers). As follows from the above consideration, it is application of such fibers that may permit one to reduce the influence of the deleterious effects limiting the average power of double-clad lasers.

    a. A promising approach which may in some cases bring about an increase in the average output power of fiber lasers lies in the use of multi-mode cores. Our analysis permits a conclusion that spatial competition among the various types of core oscillations may result in a substantial decrease of the number of lasing modes. Despite a certain increase of the output beam divergence in these conditions, such lasers will undoubtedly find application.

    b. A multi-core fiber laser with single-mode doped cores arranged in the peripheral part of the cladding which guides the pump appears promising. In such lasers, the output power increases with increasing number of parallel lasing channels. The potential of increasing the brightness of such lasers has not yet been exhausted. This problem, in particular, is associated with a number of purely technological difficulties.

References

1. J. Hecht, “Fiber Lasers Prove Versatile” // Laser Focus World, vol. 34, No 7 (1999)

2. L. Zenteno, “High Power Double-Clad fiber Lasers” // J. of Lightwave Technology, vol. 1, pp. 1435 - 1446 (1993)

3. V. P. Gapontsev, I. E. Samartsev, V. Fomin, N. S. Platonov, S. V. Chernikov, J. R. Taylor, “High power fiber laser - the revitalization of laser technology” // LEOS’ 97 Proceedings, vol. 2, p. 380 (1997)

4. D. C. Hanna, R. M. Percival, I. R. Peny, R. G. Smart, P. J. Suni, A. C. Tropper, “Yb-doped monomode fiber laser: broadly tunable operation from 1.010 /irn to 1.162 /im and a three level operation at 974 îì” // J. Modern Optics, vol. 37, pp. 329 – 331 (1987)

5. J. R. Armitage, R. Wyatt, B. J. Ainslic, S. P. Craig-Ryan, “An Yb’+-doped silica fiber laser” // Electron Lett., vol. 25, pp. 298-299 (1989)

6. J. Y. Allain, M. Monerie, H. Poignant, “Ytterbium-doped fluoride fiber laser operating at 1.02 μm” // Electron. Lett., vol 28, pp. 988-989 (1992)

7. C. J. Mackechnie, W. L. Bames, D. C. Hanna, J. E. Townsend, “High-power ytterbium-doped fiber laser operating in the 1.12 μm region” // Electron. Lett., vol. 29, pp. 52-53, 1993

8. J. Y. Allain, J. F. Bayon, M. Monerie, P. Bemage, P. Niay, “Ytterbium-doped silica fiber laser with intracore Bragg grating operating at 1.02 μm” // Electron. Lett., vol. 29, pp. 309-310 (1993)

9. P. St. J. Russell, J. L. Archambault, L. Reekie, “Fiber gratings” // Phys. World, pp. 41 – 46, Oct. 1993

10. C. J. Koestler, E. Snitzer, “Amplification in a Fiber Laser” // Applied Optics, vol. 3, pp1182-1186 (1964)

11. M. J. Digonnet, C. J. Gaeta, “Theoretical analysis of optical fiber laser amplifiers and oscillators” // Applied Optics, vol. 24, pp. 333 – 342 (1985)

12. C. L. Tang, H. Statz, G. De Mars, “Spiking behavior of solid-state lasers” //J. Appl. Physics, v. 34, p. 2289 (1963)

13. H. Statz, C. L. Tang, “Multimode oscillation in solid state masers” // J. Appl. Physics, v. 35, p. 1377 (1964)

14. Yu. A. Anan’ev, B. M. Sedov, “Spectral and temporal characteristics of Ca F2 : Sm2+ stimulated emission” // J. Exp. and Theor. Phys. (Soviet JETP), vol. 48, p. 782 (1965)

15. B. L. Livshits, V. N. Tsikunov, “Spectral properties of stimulated emission in broad pumping interval” // // J. Exp. and Theor. Phys. (Soviet JETP), vol. 49, p. 1843

(1965)

16. Yu. A. Anan'ev, "Intensity distribution of radiance of solid-state laser with plane mirrors on transverse modes" // J. of Techn. Phys., vol. 37, pp. 139-149 (1967)

17. K. Kubodera, K. Otsuka, "Single-Transverse-Mode Li Nd P4 O12 Slab Waveguide Laser" // J. Appl. Phys., vol. 50, pp. 653 – 659 (1979)

18. Yu. A. Anan'ev, O. A. Shorokhov, "Efficiency of exciting energy transformation in laser resonators" // Journal "Optiko-mekhanicheskaya promyshlennost' ", ¹ 11, pp. 12-16 (1977)

19. Yu. A. Anan'ev, S. G. Anikichev, "Quasi-stationary multi-mode oscillation in stable resonators with round mirrors" // Optika i spektroskopiya, vol. 67, pp. 693-696 (1989)

20. Yu. A. Anan'ev, E. A. Korolev, "Distribution of pumping radiation in laser crystal" // Optika i spektroskopiya, vol. 16, pp. 702-704 (1964)

21. L. Goldberg, J. P. Koplow, R. P. Moeller, D. A. Kliner, "High-power superfluorescent source with a side-pumped Yb-doped double-clading fiber" // Optics Letter, vol. 23, pp. 1037-1039 (1998)

22. L. Goldberg, J. P. Koplow, D. A. Kliner, "High efficiency 3 W side-pumped Yb fiber amplifier and laser" // CLEO '99, May 24

23. A. S. Kurkov, V. I. Karpov, A. Yu. Laptev, O. I. Medvedkov, E. M. Dianov, A. N. Gur'yanov, A. S. Vasil'ev, V. M. Paramonov, V. N. Protopopov, A. A. Umnikov, N. I. Vechkanov, V. G. Artyushenko, Yu. Fram, "High-efficient fiber laser with cladding pumping of ytterbium waveguide and fiber Bragg grating" // Kvantovaya Electronika (Quantum Electronics), vol. 27, pp. 239-240, (1999)

24. R. Paschotta, J. Nilsson, L. Reekie, A. C. Trooper, D. C. Hanna, "Single-frequency ytterbium-doped fiber laser stabilized by spatial hole burning" // Optics Letters vol. 22, pp. 40-42 (1997)

25. A. Liu, K. Ueda, "The absorption characteristics of circular, offset, and rectangular double-clad fibers" // Optics Communications vol. 132, pp. 511-518 (1996)

26. H. M. Pask, R. J. Carman, D. C. Hanna, A. C. Tropper, C. J. Mackechni, P. R. Barber, J. M. Dawes, "Ytterbium-Doped Silica Fiber lasers: Versatile Sources for the 1 - 1.2 μm Region" // IEEE J. of selected topics in Quantum Electronics vol. 1, pp. 2-13 (1995)

27. E. M. Dianov et al // Kvantovaya Electronika (Quantum Electronics), vol. 24, pp. 3-4 (1997)

28. G. Meltz, W.W. Morey, and W.H. Glenn,"Formation of Bragg gratings in optical fibers by transverse holographic method" // Opt. Lett., vol.14, no.15, pp. 823-825, 1989.

29. E. Mayer and D. Basting // Laser Focus World, pp. 107-110, April 2000.

30. R.H. Stolen and E.P. Ippen // Appl.Phys.Lett., vol. 22, p. 276 (1973).

31. R. Stolen and C. Lin, CRC Handbook of Laser Science and Technology, Supplement 1: Lasers // M. J. Weber, ed., CRC Press, Boca Raton, FL (1991).

32. S.G. Grubb and A.J. Stentz // Laser Focus World, “Fiber Raman lasers emit at many wavelengths,” vol.32, no.2, February, 1996.

33. S.G. Grubb et al. // OSA Topical Meeting: Optical Amplifiers and Their Applications, paper SaA4, Davos, Switzerland (1995).

34. Ilko K. Ilev, Hiroshi Kumagai, and Koishi Toyoda, “widely tunable (0.54 –1.0 μm) double-pass fiber Raman laser” // Appl. Phys. Lett. , vol. 69(13), pp. 1846-1848 (1996).

35. Do Il Chang, S.V. Chernikov, M.J. Guy, J.R. Taylor, Hong Jin Kong, “Efficient cascaded Raman generation and signal amplification at 1.3 μm in GeO2-doped single-mode fiber” // Optics Communications, vol. 142, pp. 289-293(1997)

36. S.V. Chernikov, Y. Zhu, R. Kashyap, J.R. Taylor // Electron. Lett. , vol. 31, pp. 472 (1995)

37. P.B. Hansen, A.J. Stentz, L. Eskilden, S.G. Grubb, T.A. Strasser, J.R. Pedrazzani, Electron. Lett. , vol. 32, p. 2164 (1996)

38. E.M. Dianov, M.V. Grekov, I.A. Bufetov, S.A. Vasiliev, O.I. Medvedkov, V.G. Plotnichenko, V.V. Koltashev, A.V. Belov, M.M. Bubnov, S.L. Semjonov and A.M. Prochorov, “CW high power 1.24 μm and 1.48 μm Raman lasers based on low loss phosphosilicate fiber” // Electron.Letts, vol. 33, p. 1542 (1997)

39. ? .? .??????, ? .? .??? ????, ? .? .??????, ? .?.?????? ? ??. “? ?????????? ???????? ? ???????? ???-????? (λ=1.24 ???) ?? ????????????? ?????????”, ????????? ???????????, ?. 29, ? 2, ???. 97-100 (1999)

40. Uwe Brinkmann, “FIBER LASERS: Upconversion enhances blue emission” // Laser Focus World, vol. 36, no.1, January, 2000

41. H.M. Pask, A.C. Topper, D.C. Hanna, B.N. Samson, R.D.T. Lauder, P.R. Barber, L. Reekie, J.L. Archambault, S.T. Davey, and D. Szebesta, “Upconversion laser action in Pr3+-doped ZBLAN fiber pumped by an Yb-doped silica fiber laser” // Adv. Solid-State Lasers, Salt Lake City, UT. Tech. Dig., paper AtuD1-1, , pp. 172-174 (1994)

42. P.R. Barber, C.J. Mackechnie, R.D.T. Lauder, H.M. Pask, A.C. Topper, D.C. Hanna, S.D. Butterworth, M.J. McCarthy, J.L. Archambault, and L. Reekie, , S.T. Davey, and D. Szebesta, “All solid-state blue room temperature Thulium-doped upconversion faber laser” // Compact Blue-Green Lasers, Salt Lake City, UT. Tech. Dig., paper CFA3-1, pp. 68-70. (1994)

43. H. Zellmer, P. Riedel, and A. Tennermann // App. Phys., vol. B69(5/6), p.417 (1999)

44. Paul Mortensen, “Diode-pumped fiber laser produces 1 mW at 492 îì” // Laser

Focus World, vol. 32, no. 11 (1996)

45. Lawrence E. Myers, Walter R. Bosenberg // IEEE J. Quantum Electron., vol. 33, no. 10, pp. 1663-1672 (1997)

46. “Periodically poled lithium niobate efficiently doubles modelocked fiber-laser output” // Laser Focus World, vol. 33, no.3 (1977)

47. S.A. Guskov, S. Popov, S.V. Chernikov and J.R. Taylor, ”Second harmonic generation around 0.53μm of seeded Yb fiber system in periodically-poled lithium niobate” // Electronics Letters Online No: 19980987, 18 May 1998

48. P.E. Britton, D. Taverner, K. Puech, D.J. Richardson, P.G.R. Smith, G.W. Ross, and D.C. Hanna, “Optical parametric oscillation in periodically poled lithium niobate driven by a diode-pumped Q-switched erbium fiber laser” // Optics Letters, vol. 23, No. 8, pp.582-584 (1998)

49. P. E. Britton et al. // Technical Digest CLEO `98, paper CTuK4 (San Francisco, CA, 1998).

50. N. J. Traynor et al. // Technical Digest CLEO `98, paper CTuK6 (San Francisco, CA, 1998).

51. ? .? .??? ????, ? .?.??????, ? .? .??????, ? .? .??????, ?.?.??????, “? ?????????? ???????? ?????????? ?? ?????? ?? ????????? ?? ?????????? ??????, ???????????? ??????” // «????????? ??????????», ?. 25, ? 4, ???. 348-350 (1998)

52. ??????? ? .? ., ? ?????? ?.? ., ? ?? ?.?., ????????? ?.?., ????? ?.? ., ? ?????? ???????????????? ?????????? ?????????? ?????????? // ? ? ? ? , ?. 44, ?. 1884 - 1888 (1963)

53. Rigrod W., Gain saturation and output power of optical masers // J. Appl. Phys., v. 34, p. 2602 (1963)

54. A. S. Kurkov, V. I. Karpov, A. Yu. Laptev, O. I. Medvedkov, E. M. Dianov, A. N. Gur’yanov, A. S. Vasil’ev, V. M. Paramonov, V. N. Protopopov, A. A. Umnikov, N. I. Vechkanov, V. G. Artyushenko, Yu. Fram, “High-efficient fiber laser with cladding pumping of ytterbium waveguide and fiber Bragg grating” // Kvantovaya Electronika (Quantum Electronics), vol. 27, pp. 239-240, (1999)

55. L. Goldberg, J. P. Koplow, R. P. Moeller, D. A. Kliner, “High-power superfluorescent source with a side-pumped Yb-doped double-cladding fiber” // Optics Letter, vol. 23, pp. 1037-1039 (1998)

56. H. L. Kelley, “Self-focusing of optical beams”, Phys. Rev. Lett., vol. 15, no. 26, p. 1005 (1965)

57. A. Girard, Litewave, July 2000, p. 84

58. D.C. Hanna, M.J. McCarthy, and P.J. Suni, “Thermal considerations in longitudinally pumped fiber and miniature bulk lasers,” SPIE, vol. 1171, Fiber Laser Sources and Amplifiers (1989) 160.

59. E. Snitzer, “Glass lasers,” Appl. Opt., vol. 5, no. 10, 1966, p. 1487

60. Anping Liu, Kenichi Ueda, “The absorption characteristics of circular, offset, and rectangular double-clad fibers” Opt. Comm., 132 (1996) 511-518.

61. M. E. Fermann, Opt. Lett. **23**, 52 (1998)

62. M.E. Fermann, M.L. Stock, A. Galvanauskas, D.J. Harter, “High-power compact ultrafast fiber laser” Proc.SPIE Vol. 3942, p. 194-200, April 2000

63. M.E. Fermann, A. Galvanauskas, M.L. Stock, K.K. Wong, D. Harter, and L. Goldberg, Opt. Lett. **24**, 1428 (1999).

64. G. C Cho, A. Galvanauskas, M. E. Fermann, M. L. Stok, D. Halter “100μJ and 5.5. W Yb-fiber femtosecond chirped pulse amplifier system” CLEO-2000 p.118, May 2000.

65. A. Galvanauskas, M. E. Fermann “13-W average power ultrafast fiber laser” Optics & Photonics News, Volume 11, Issue 8, August 2000, pp 41-42.

66. http://www.ieee.org/organizations/pubs/newsletters/leos/aug00/high.htm

67. Sung-Hak Cho, Hiroshi Kumagai, Katsumi Midorikawa, Minoru Obara, “Fabrication of double cladding structure in optical multimode fibers using plasma channeling excited by a high-intensity femtosecond laser” Optics Communications v.168, pp.287–295,September 1999.

68. D. Gloge, Weakly Guiding Fibers, Applied Optics/October 1971/Vol. 10, No. 10, p 2252-2258.

69. Salvatore Solimeno, Bruno Crosignani, Paolo DiPorto, Guiding, Diffraction, and Confinement of Optical Radiation, 1986, Academic Press, Inc., Harcourt Brace Jovanovich, Publishers.

70. M.J.F. Digonnet and C.J.Gaeta,”Theoretical analysis of optical fiber laser amplifiers and oscillators,”Appl. Opt. 24, 113 (1985).

71. Anthony E. Siegman, “Lasers”, University Science Books, 1986

72. P. Glass, M. Naurmann, A. Schirrmacher, Th. Pertsch “The multicore fiber – a novel design for a diode pumped fiber laser” Optics Communications v.151, pp.187-195, May 1998.

73. A. Galvanauskas, M. E. Fermann “13-W average power ultrafast fiber laser” Optics & Photonics News, Volume 11, Issue 8, August 2000, pp 41-42.

74. A.W. Snyder, J.D. Love, Optical waveguide Theory, Chapman and Hall, 1983

75. Kin S. Chiang, “Intermodal dispersion in two-core optical fibers” Optics Letters, Vol. 20, No. 9, p. 997-999, May 1995.

76. N.N. Elkin, A.P. Napartovich, A.G. Sukharev, V.N. Troschieva, D.V. Vysotsky “Direct numerical simulation of radiation propagation in a multicore fiber” Optics

Communications 177 (2000) pp. 207-217.

77. B. Ozygus, Ph. Thesis. Technical University Berlin, 1995

78. V.P. Kalinin, D.A. Goryachkin, V.M. Gromovenko, N.A. Romanov, A.Yu. Rodionov, S.A. Dimakov, V.M. Irtuganov, V.I. Kuprenyuk, V.E. Sherstobitov, Yu.A. Rezunkov, “Feasible configurations of a repetitively pulsed TEA CO2 laser with small angular divergence and 1- kJ pulse energy” Proc. SPIE Vol. 3574, p. 187-202, December, 1998

79. H.J. Eichler, B. Liu, O. Mehl “Application of fiber phase conjugators in high power lasers”, Proc. SPIE Vol. 3549, p. 110-113, September, 1998

80. Yu.V. Miklyaev, V.I. Safonov, “Beam and fiber coupled by phase conjugation” Proc. SPIE Vol. 3488, p. 220-224, October, 1997.

81. P. Delae, A. Fotiadi, G. Roosen, “Reciprocity and phase conjugation: application to the study of the double phase conjugate mirror”, Optics Communications v.174, pp. 257-269, 2000.

82. H.J. Eichler, B. Liu, O. Wittler, Q. Zhu “Fiber phase conjugators with a saturated SBS reflectivity” Proc. SPIE Vol. 3549, p. 114-117, September, 1998.

83. I.M. Beldiugin, M.G. Galushkin, M.V. Zolotarev, F.F. Kamenets, “Phase conjugation in a ring resonator with a four-wave mirror” Izvestiya Akademii Nauk SSSR Seriya Fizicheskaya vol51,Feb.1987, pp.358-361 (In Russian)

84. ? .? . ??????? «?????????? ?????????? ? ???????? ???????????? ????????? ?????????» ???. 308 ? ????? «? ????» 1979.

85. M. Zdeblick “Design variables prevent a single indastry standard” Laser Focus World, March 2001

86. N.A. Gryaznov, V.Yu. Kiselev «Linear conjugate phase-locking of independent single-mode emitters” QE v.30, p. 421, 2000.

87. S.J.Brosnan, L.O. Heflinger, D.G. Heflinger, “Improved high average power fiber laser system with high-speed, parallel wavefront sensor” Patent TRW INC (US), EP1041686, 4 October 2000.